iScience

CellPress
OPEN ACCESS

Article

LncRNA *IRAIN* overcomes imatinib resistance in chronic myeloid leukemia via NF-κB/CD44 pathway inhibition

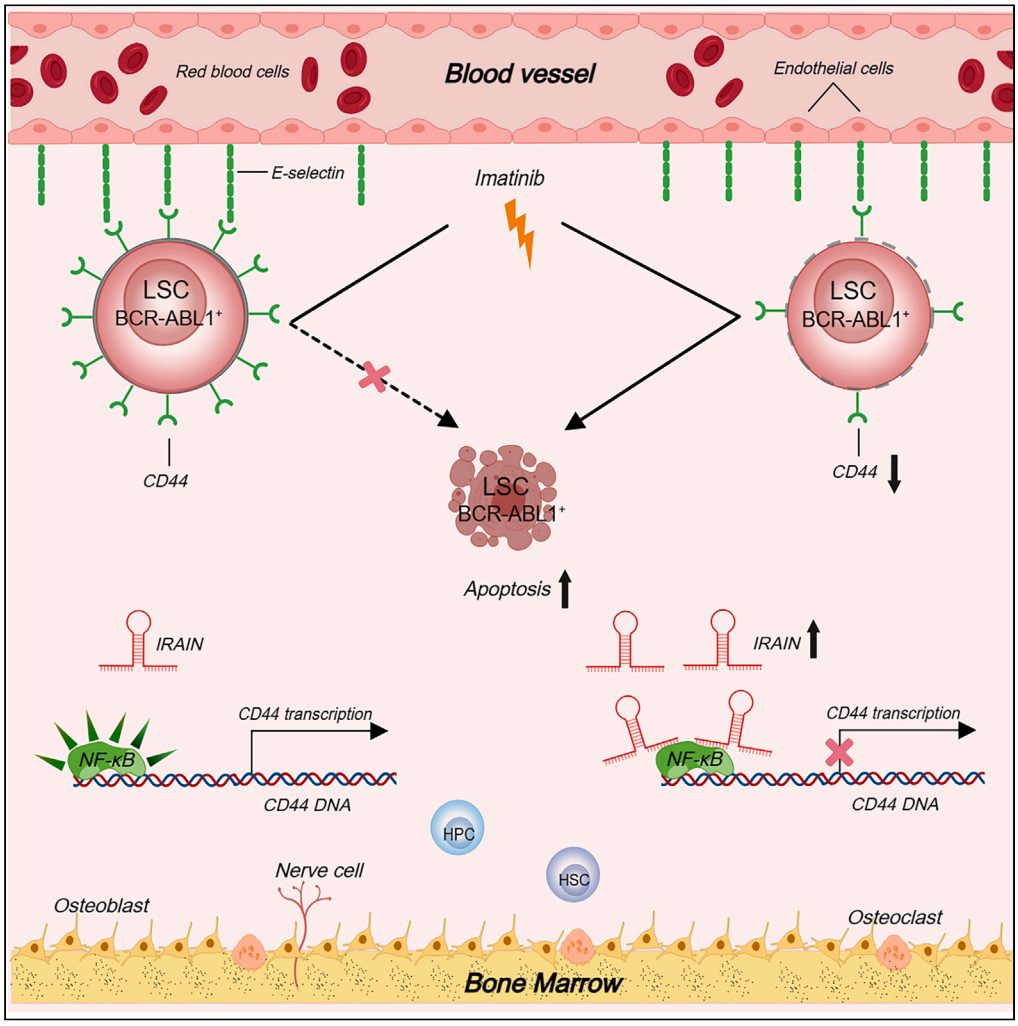

Xijia Wang, Yutong Hou, Yizhu Lyu, ..., Fang Xie, Xuehong Zhang, Jinsong Yan

xiefang5105@163.com (F.X.)
zhangxuehong1984@163.com (X.Z.)
yanjsdmu@dmu.edu.cn (J.Y.)

Highlights

Low expression of IRAIN resulted in imatinib resistance in chronic myeloid leukemia

IRAIN inhibits CD44 through binding to NF-κB subunit p65 and reducing p65

Decitabine overcomes imatinib resistance by upregulation of IRAIN

IRAIN can be a potential therapeutic target in chronic myeloid leukemia

Wang et al., iScience 27, 109851
June 21, 2024
https://doi.org/10.1016/j.isci.2024.109851

iScience

CellPress
OPEN ACCESS

Article

LncRNA *IRAIN* overcomes imatinib resistance in chronic myeloid leukemia via NF-κB/CD44 pathway inhibition

Xijia Wang,[1,2,5] Yutong Hou,[1,5] Yizhu Lyu,[1,5] Jiayin Zhou,[1,2] Xin Zhang,[1,2] Mohammad Arian Hassani,[1,2] Dan Huang,[1,2] Zhijia Zhao,[1] Dong Zhou,[1] Fang Xie,[1,2,*] Xuehong Zhang,[3,*] and Jinsong Yan[1,2,4,6,*]

SUMMARY

The development of tyrosine kinase inhibitors (TKIs) has revolutionarily increased the overall survival of patients with chronic myeloid leukemia (CML). However, drug resistance remains a major obstacle. Here, we demonstrated that a BCR-ABL1-independent long non-coding RNA, *IRAIN*, is constitutively expressed at low levels in CML, resulting in imatinib resistance. *IRAIN* knockdown decreased the sensitivity of CD34$^+$ CML blasts and cell lines to imatinib, whereas *IRAIN* overexpression significantly increased sensitivity. Mechanistically, *IRAIN* downregulates CD44, a membrane receptor favorably affecting TKI resistance, by binding to the nuclear factor kappa B subunit p65 to reduce the expression of p65 and phosphorylated p65. Therefore, the demethylating drug decitabine, which upregulates *IRAIN*, combined with imatinib, formed a dual therapy strategy which can be applied to CML with resistance to TKIs.

INTRODUCTION

Chronic myeloid leukemia (CML) is characterized by the BCR-ABL1 fusion oncoprotein with a constitutive tyrosine kinase activation yielded by chromosomal translocation t(9; 22) (q34; q11.2).[1,2] Its frontline therapeutic agents include tyrosine kinase inhibitors (TKIs).[3] The first approved imatinib mesylate revolutionized CML treatment by improving the 10-year survival rate from less than 20% to around 83%.[4,5] The outstanding prolongation of overall survival results from deep molecular responses (DMRs). For instance, patients with CML on TKI therapy that reached response milestones of ≤10% *BCR-ABL1* transcripts by three months, ≤1% by six months, or ≤0.1% by 12 months on the international scale (IS) commonly have good prognoses.[6,7] Furthermore, patients who achieve a DMR of 4.5 (*BCR-ABL1* transcripts with a 4.5-log reduction)[8] from a standardized baseline lasting for over two years may meet the criteria for discontinuing TKIs.[6,9,10] However, approximately 17% of patients with CML develop imatinib resistance during a five-year follow-up.[11] Although second and third-generation TKIs are effective against most instances of drug resistance due to BCR-ABL1 kinase domain mutations, they cannot overcome resistance from other causes, such as activation of BCR-ABL1-independent pathways.[12] Therefore, potential strategies are in demand to overcome TKI resistance.

Leukemic stem cells (LSCs) in bone marrow are commonly associated with drug resistance in varied therapeutic agents, resulting in incurable and relapsed hematological malignancies.[13–16] A classical biomarker of a healthy hematopoietic stem cell, CD44, is broadly expressed on LSCs, and a higher expression level of CD44 generally predicts a worse prognosis in leukemia cases.[17,18] CD44 plays a key role in regulating adhesion, migration, and homing of the hematopoietic stem cells in CML.[19] Highly expressed CD44 molecules bind to its ligand E-selectin on endothelial cells, enabling LSCs to reside in the marrow environment in a quiescent state, preventing the LSCs of CML from being eradicated by TKIs.[16] Moreover, the dissociation of CD44 from E-selectin may re-sensitize LSCs to TKIs.[16,20] Thereby, CD44 may be a potential therapeutic target for overcoming TKI resistance in CML.

Accumulating evidence has revealed that a few long non-coding RNAs (lncRNAs), such as *NEAT1*[21] and *MEG3*,[22,23] are closely implicated in tumorigenesis and drug resistance in CML. *IRAIN*, an intragenic antisense lncRNA, was first discovered within the insulin-like growth factor type I receptor (*IGF1R*) promoter complex in 2014.[24] *IRAIN* has contradictory effects on various cancer types. For instance, it serves as a tumor suppressor in acute myeloid leukemia (AML) because it inhibits cell migration, and its high expression is associated with a low risk of leukemia.[24] The intragenic activation decreased cell proliferation, tumor sphere formation, migration, and invasion by inhibiting the IGF1R signaling pathway in breast cancer.[25] Moreover, *IRAIN* is involved in modulating drug resistance in treating gliomas, in which the overexpression of *IRAIN* reversed the resistance to temozolomide.[26] However, one study revealed that *IRAIN* functioned as a risk factor for cancer

[1]Department of Hematology, Liaoning Medical Center for Hematopoietic Stem Cell Transplantation, the Second Hospital of Dalian Medical University, Dalian 116027, China
[2]Liaoning Key Laboratory of Hematopoietic Stem Cell Transplantation and Translational Medicine, Blood Stem Cell Transplantation Institute, Dalian Key Laboratory of Hematology, Diamond Bay Institute of Hematology, the Second Hospital of Dalian Medical University, Dalian 116027, China
[3]Center of Genome and Personalized Medicine, Institute of Cancer Stem Cell, Dalian Medical University, Dalian, Liaoning 116044, China
[4]Department of Pediatric, Pediatric Oncology and Hematology Center of the Second Hospital of Dalian Medical University, Dalian, Liaoning 116027, China
[5]These authors contributed equally
[6]Lead contact
*Correspondence: xiefang5105@163.com (F.X.), zhangxuehong1984@163.com (X.Z.), yanjsdmu@dmu.edu.cn (J.Y.)
https://doi.org/10.1016/j.isci.2024.109851

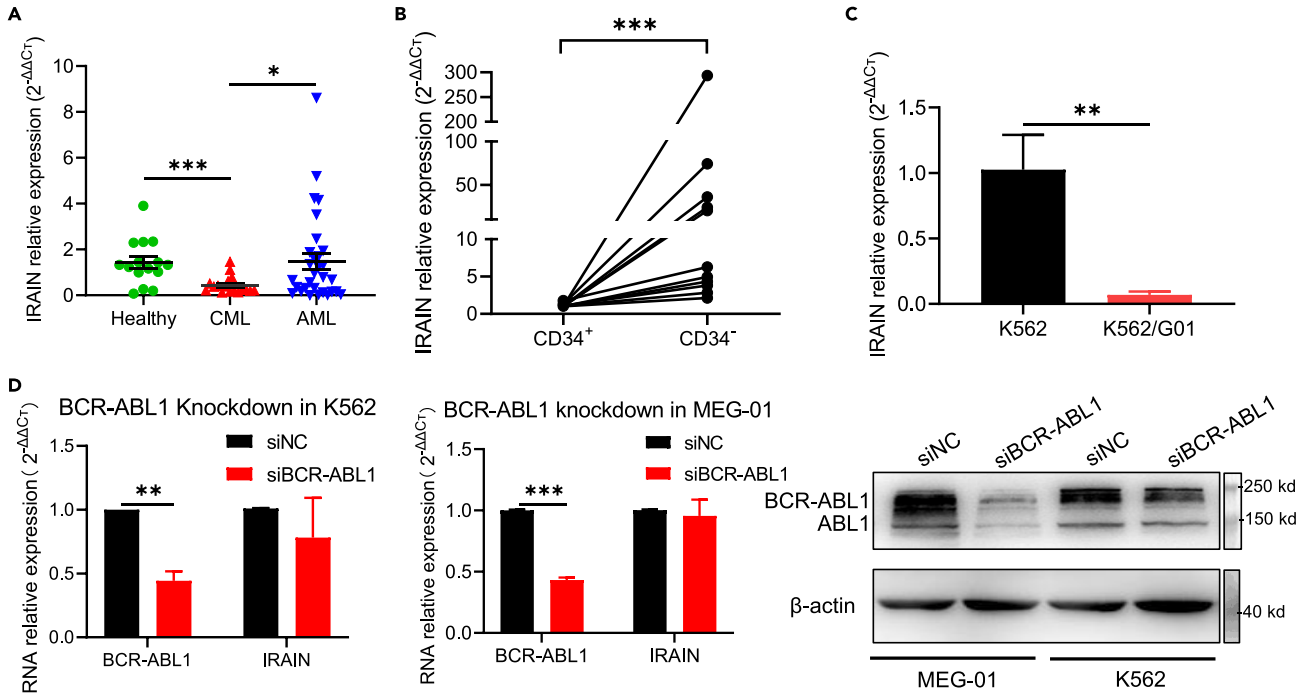

Figure 1. Low constitutive expression of *IRAIN* is associated with imatinib resistance, independent of BCR-ABL1, in CML

(A) *IRAIN* expression levels were measured in healthy volunteers (N = 15) and patients with newly diagnosed CML (N = 17) and AML (N = 30) using qRT-PCR. *GAPDH* was used as a reference gene.

(B) *IRAIN* levels were measured in $CD34^+$ and $CD34^-$ cells from patients with CML (N = 9) using qRT-PCR. Each line represents samples from the same patient.

(C) *IRAIN* levels in imatinib-sensitive K562 cells and resistant K562/G01 cells were measured using qRT-PCR. Data are represented as mean ± SD of three technical replicates.

(D) In K562 and MEG-01 cells, *IRAIN* was knocked down with siRNA against BCR-ABL1 (siBCR-ABL1) and the negative control siRNA (siNC). *IRAIN* and BCR-ABL1 transcripts were detected using qRT-PCR (Left), and BCR-ABL1 protein levels were detected using western blotting (Right) 48 h after transfection. The qRT-PCR data are represented as mean ± SEM of three independent experiments. Differences in expression between groups(A, B, C. and D) were calculated by unpaired t test. *$p < 0.05$, **$p < 0.01$, ***$p < 0.001$. Also, see Figure S1 and Table S1.

development. *IRAIN* inhibited apoptosis and promoted cell proliferation by interacting with the *EZH2* enhancer, LSD1, in pancreatic cancer.[27] However, the function of *IRAIN* in resistance to TKI remains unknown in CML.

In this study, the constitutive expression of *IRAIN* was low and was associated with imatinib resistance in CML. When *IRAIN* was overexpressed, it overcame imatinib resistance by downregulating CD44 via inhibiting the NF-κB/CD44 axis in CML cells. Furthermore, the demethylation agent, decitabine (DAC), increased *IRAIN* expression and reversed imatinib resistance in CML cells. Therefore, this study suggests that *IRAIN* may reduce drug resistance to TKIs, independent of the BCR-ABL1 oncoprotein in CML cells.

RESULTS

Low constitutive expression of *IRAIN* is associated with imatinib resistance, independent of BCR-ABL1, in CML

A previous study reported that the *IRAIN* promoter is completely methylated in CML cell lines and semi-methylated in patients with AML and healthy volunteers.[24] However, the expression levels of *IRAIN* in patients with CML or AML and healthy volunteers remain unclear. Therefore, *IRAIN* expression levels were detected using qRT-PCR in the bone marrow mononuclear cells (BMMNCs) of 17 patients with CML, 30 patients with AML, and 15 healthy volunteers (Figure 1A). Information of human participant was listed in Table S1. The expression of IRAIN was the lowest in CML and intermediate in AML. The expression of *IRAIN* was much lower in patients with CML than in healthy volunteers (***$p = 0.0006 < 0.01$) and in patients with AML (*$p = 0.033 < 0.05$). There was no statistical difference in *IRAIN* expression between AML and healthy volunteers. Meanwhile, $CD34^+$ cells were immunomagnetically sorted from nine CML samples (Figure S1A). The expression of *IRAIN* was significantly decreased in CML $CD34^+$ cells compared to that in CML BM mononuclear cells (Figure 1B), suggesting that the constitutive expression of *IRAIN* was lower in $CD34^+$ leukemia stem cells than in primary blast cells in CML.

IRAIN is associated with resistance to chemotherapy in glioma.[28] However, the association of *IRAIN* with drug resistance in leukemia needs to be clarified. Therefore, an imatinib-resistant cell line, K562/G01, was used to test whether *IRAIN* expression can contribute to imatinib resistance in CML. The proliferation rates between K562/G01 and control cells, K562 cells, were equal (Figure S1B); however, addition of 1.0 μM imatinib inhibited the proliferation of K562 cells but did not affect the proliferation of K562/G01 cells (Figure S1C), indicating that K562/G01

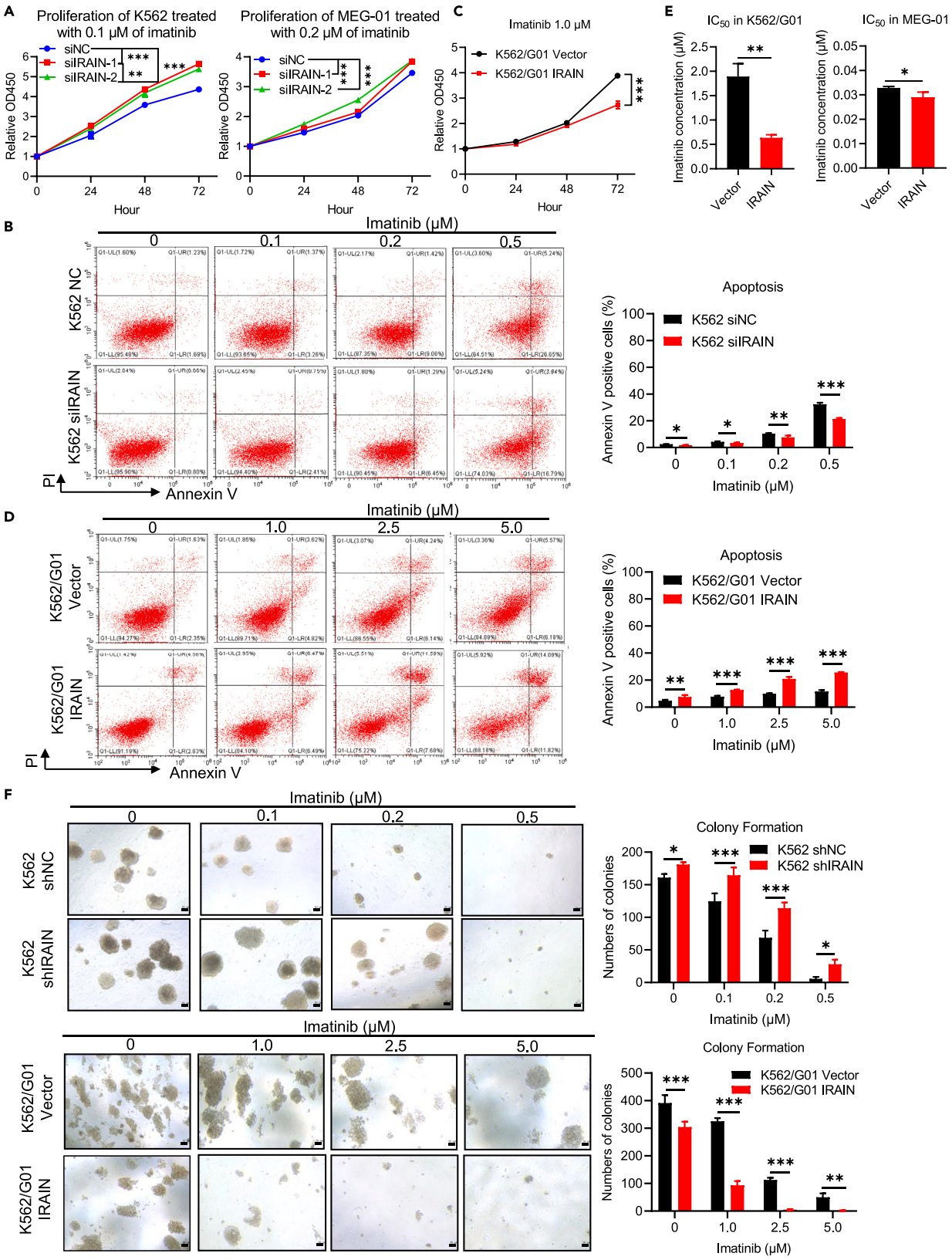
A
Proliferation of K562 treated with 0.1 μM of imatinib
Proliferation of MEG-01 treated with 0.2 μM of imatinib
siNC
siIRAIN-1
siIRAIN-2
Relative OD450
Hour
C
Imatinib 1.0 μM
K562/G01 Vector
K562/G01 IRAIN
E
IC50 in K562/G01
IC50 in MEG-01
Imatinib concentration (μM)
Vector
IRAIN
B
Imatinib (μM)
K562 NC
K562 siIRAIN
PI
Annexin V
Apoptosis
K562 siNC
K562 siIRAIN
Annexin V positive cells (%)
D
K562/G01 Vector
K562/G01 IRAIN
F
K562 shNC
K562 shIRAIN
Colony Formation
Numbers of colonies

Figure 2. Knockdown of *IRAIN* resulted in imatinib resistance in CML cell lines

(A) *In vitro* proliferation of K562 or MEG-01 cells transfected with two siRNAs against *IRAIN* (siIRAIN) and a negative control siRNA (siNC) was determined using the CCK8 assay after treatment for 0, 24, 48, and 72 h with indicated concentrations of imatinib. Data are represented as mean ± SD of three biological replicates.

(B) Cell apoptosis was measured using flow cytometry after Annexin V/PI dual staining of K562 cells transfected with a siRNA against *IRAIN* (siIRAIN) and a negative control siRNA (siNC) after treatment for 48 h with indicated concentrations of imatinib. Data are represented as mean ± SEM of three biological replicates.

(C and D) Proliferation of K562/G01 cells stably expressing *IRAIN* (K562/G01 IRAIN) or the vector (K562/G01 Vector) was determined using the CCK8 assay after treatment for 0, 24, 48, and 72 h with 1.0 μM of imatinib, and (C) Cell apoptosis was measured using flow cytometry after Annexin V/PI dual staining in these cells treated with indicated concentrations of imatinib for 48 h.

(E) *IRAIN*-overexpressing K562/G01 and MEG-01 cells were treated with gradient concentrations of imatinib for 48 h. Cell viability was determined using the CCK8 assay, and the IC_{50} values were analyzed using a non-linear regression curve with Prism 8 software. Data are represented as mean ± SEM of three biological replicates.

(F) *IRAIN*-knockdown K562 cells (K562 shIRAIN) and control K562 (K562 shNC) were used to observe the colony forming ability. 14 days after addition of imatinib at concentrations of 0 μM, 0.1 μM, 0.2 μM, 0.5 μM, the number of colonies were counted under light microscope. *IRAIN*-overexpressing K562/G01 cells (K562/G01 IRAIN) and the K562/G01 cells transfected with vector (K562/G01 Vector) served as control were used to observe the colony forming ability. 14 days after addition of imatinib at concentrations of 0 μM, 1.0 μM, 2.5 μM, 5.0 μM, the number of colonies were counted under light microscope. Representative pictures of colonies with ≥50 cells are shown. Scale bar represents 50 μm. Three independent experiments are quantified. Differences in proliferation rates (A and C), apoptosis levels (B and D), IC_{50} concentrations (E) between groups were calculated by unpaired t test. Differences in numbers of colonies (F) were calculated by One-way ANOVA.*$p < 0.05$, **$p < 0.01$, ***$p < 0.001$. Also, see Figure S2.

cells were resistant to imatinib. Resistance was also confirmed by measuring the half-maximal drug inhibitory concentration (IC_{50}) in both cells. The IC_{50} of imatinib in K562/G01 cells was ten times higher than that in K562 cells (Figure S1D). *IRAIN* expression was lower in K562/G01 cells than in K562 cells (**$p = 0.0034 < 0.01$, Figure 1C), suggesting that *IRAIN* expression is associated with imatinib resistance in CML cell lines.

BCR-ABL1 is a leukemogenesis driver and a therapeutic target inhibited by imatinib. The association between *IRAIN* and imatinib resistance was identified using K562/G01 cells. We further assessed whether *IRAIN* was regulated by BCR-ABL1 oncoprotein to better understand the role of *IRAIN* and imatinib resistance. *In vitro* studies showed that *BCR-ABL1* transcripts were knocked down with small interfering RNA (siRNA) in K562 and MEG-01 cells, which led to reductions in BCR-ABL1 transcription by over 50% in both cells (**$p < 0.01$, K562 cells; ***$p < 0.001$, MEG-01 cells) as detected using qRT-PCR and reduced protein levels of BCR-ABL1 detected using western blotting (Figure 1D). The transcriptional expression of *IRAIN* remained stable in BCR-ABL1-knockdown K562 and MEG-01 cells (Figure 1D), indicating that the association between *IRAIN* and imatinib resistance was independent of the BCR-ABL1 oncoprotein.

Knockdown of *IRAIN* resulted in imatinib resistance in CML cell lines

Low *IRAIN* expression is whether a causative factor of imatinib resistance or the resultant effect of imatinib resistance in CML cell lines needs to be further clarified. In the CML cell lines, K562 and MEG-01, *IRAIN* was knocked down using siRNA, as confirmed using qPCR (Figure S2A), and cell proliferation and apoptosis were analyzed after adding imatinib. Adding imatinib at a concentration of 0.1 μM led to a reduced proliferation rate in K562 siNC cells but a markedly increased proliferation in K562 siIRAIN-1 and K562 siIRAIN-2 cells (Figure 2A). Similar findings were observed in MEG-01 siNC, siIRAIN-1, and siIRAIN-2 cells (Figure 2A). *IRAIN*-knockdown K562 cells were treated with a series of concentrations of imatinib (0 μM, 0.1 μM, 0.2 μM, and 0.5 μM) for 48 h. The apoptosis rates were lower in K562 siIRAIN cells than in K562 siNC cells at each concentration of imatinib (Figure 2B). The apoptosis percentages were 2.43%, 4.20%, 10.38%, and 32.37% in K562 siNC cells and 1.67%, 3.40%, 7.58%, and 21.38% in K562 siIRAIN-1 cells at imatinib concentrations of 0, 0.1, 0.2, and 0.5 μM, respectively (Figure 2B). Similar trends in apoptosis rates were observed in MEG-01 siNC and siIRAIN-2 cells treated with imatinib for 48 h, and the concentrations of imatinib were chosen according to the IC_{50} values in MEG-01 cells (Figure S2B). The apoptosis percentages were 20.25%, 42.73%, 73.18%, and 87.17% in MEG-01 siNC cells and 9.35%, 28.64%, 66.71%, and 84.55% in MEG-01 siIRAIN-2 cells at imatinib concentrations of 0, 0.1, 0.2, and 0.5 μM, respectively (Figure S2C). These data indicate that *IRAIN* knockdown induces imatinib resistance in CML cells.

To further confirm that imatinib resistance was induced by low *IRAIN* expression, K562/G01 and MEG-01 cells were separately transfected with lentiviral plasmids to overexpress *IRAIN*, as confirmed using qRT-PCR (Figure S2D). The imatinib-resistant K562/G01 cells, induced by K562 cells, presented similar proliferation rates with no addition of imatinib but had lower *IRAIN* expression than the K562 cells. Therefore, K562/G01 cells were selected for establishing stable cell sublines overexpressing *IRAIN*, and the sublines were renamed K562/G01 Vector and K562/G01 *IRAIN*, respectively. K562/G01 *IRAIN* cells exerted significantly decreased proliferation rates compared to K562/G01 Vector cells at imatinib concentrations of 1.0 μM, 2.5 μM, and 5.0 μM (Figures 2C and S2E). As shown in Figure 2D, imatinib dose-dependently increased apoptosis rates in K562/G01 *IRAIN* cells at concentrations of 0 μM, 1.0 μM, 2.5 μM, and 5.0 μM for 48 h. Furthermore, the K562/G01 *IRAIN* cells presented higher apoptosis rates than the K562/G01 Vector cells at each corresponding concentration of imatinib (Figure 2D). Briefly, the apoptosis rates were 4.71%, 7.79%, 9.98%, and 11.54% in K562/G01 Vector cells and 7.53%, 12.63%, 20.93%, and 25.57% in K562/G01 *IRAIN* cells at imatinib concentrations of 0 μM, 1.0 μM, 2.5 μM, and 5.0 μM, respectively (Figure 2D). To confirm that the observed imatinib-induced apoptosis rates were related to *IRAIN* expression, they were compared between MEG-01 Vector and MEG-01 *IRAIN* cells in the presence of imatinib (Figure S2F). Imatinib concentrations of 0 μM, 0.1 μM, 0.2 μM, and 0.5 μM led to apoptosis rates of 3.72%, 20.09%, 49.32%, and 83.93% in MEG-01 *IRAIN* cells and 2.39%, 7.39%, 28.02%, and 63.37% in MEG-01 Vector cells, respectively (Figure S2F). Moreover, the apoptosis rates were higher in MEG-01 IRAIN cells than in MEG-01 Vector cells, suggesting that the overexpression of *IRAIN* enabled overcoming imatinib resistance in CML cell lines.

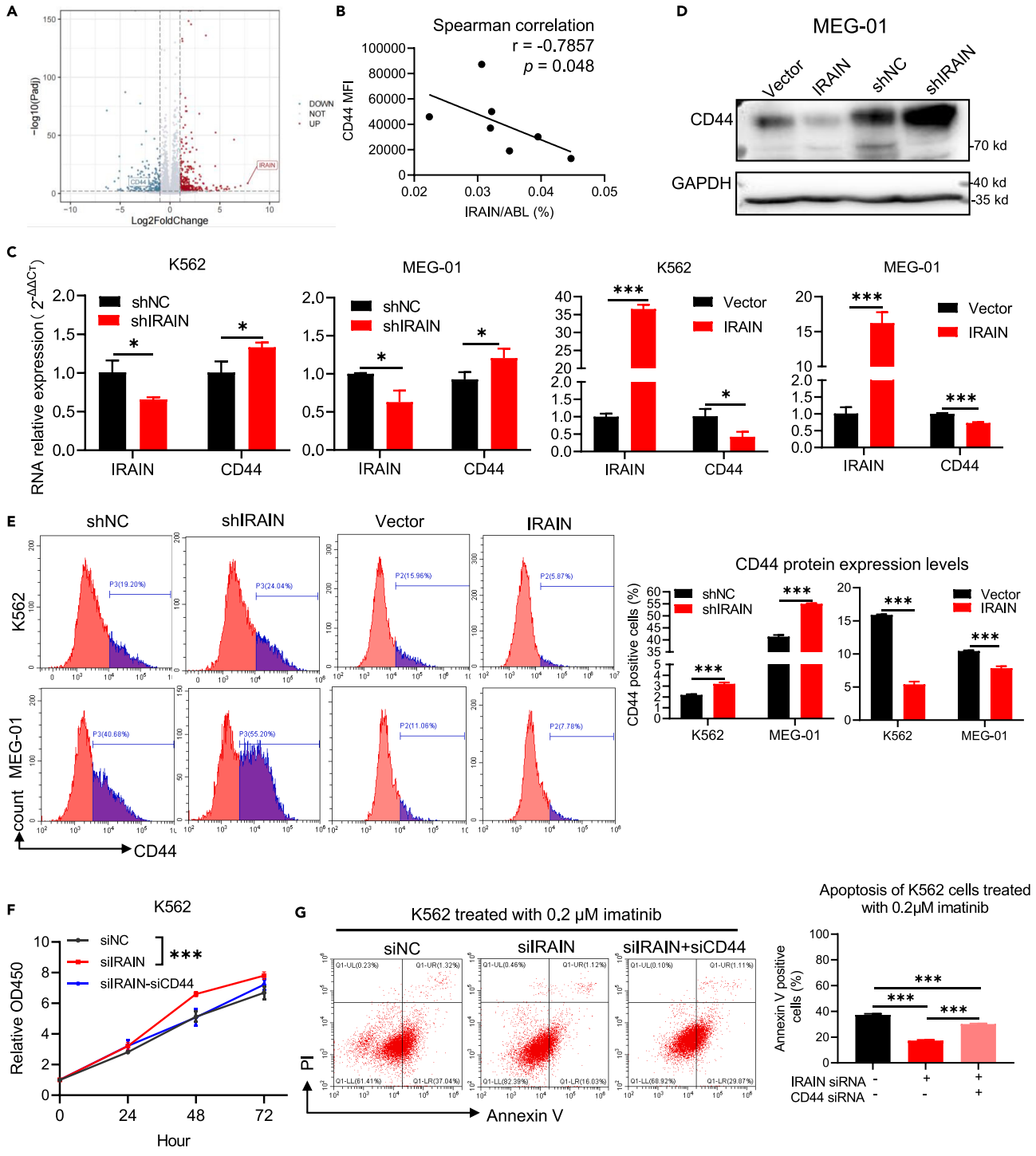

Figure 3. Imatinib resistance was overcome by *IRAIN*-downregulated CD44 expression in CML cell lines

(A) Volcano plots show differentially expressed genes between overexpressed *IRAIN* and control K562 cells (detected using RNA-sequencing analysis). Genes with changes >1.0-fold and *p*-values <0.05 were classified as significantly different.

(B) The Scatterplot and Spearman's correlation were applied to evaluate the correlation strength between the absolute expression levels of *IRAIN* and protein levels of CD44 of bone marrow mononuclear cells of patients with CML. A linear regression line helps visualize the correlation. The absolute expression levels of *IRAIN* were detected with a TaqMan-probe qRT-PCR, and CD44 surface protein levels were detected using flow cytometry, Spearman correlation r = −0.75, *$p < 0.05$.

Figure 3. *Continued*

(C) RNA levels of *IRAIN* and *CD44* were detected using qRT-PCR in transfected overexpressed *IRAIN* and knockdown cell lines of K562 and MEG-01, with *GAPDH* as the reference gene. Data are represented as mean ± SD of three technical replicates.

(D) Western blotting was used to detect the protein levels of CD44 in overexpressed *IRAIN* and knocked down MEG-01 cells, and *GAPDH* was used as a reference control protein.

(E) The CD44 protein levels of overexpressed *IRAIN* and downregulated K562 and MEG-01 cells were detected using flow cytometry. Data are represented as mean ± SEM of three biological replicates.

(F) Proliferation was detected in K562 cells transfected with the siRNA of the negative control (siNC), siRNA against *IRAIN* (siIRAIN), and siRNA against CD44 (siCD44) using CCK8 assay after transfection for 0, 24, 48, and 72 h. Data are represented as mean ± SD of three technical replicates.

(G) Apoptosis was analyzed in K562 cells transfected with siRNAs against *IRAIN* (siIRAIN), CD44 (siCD44), or no target negative control (siNC) and treated with 0.2 μM imatinib for 48 h after transfection through Annexin V/PI dual staining using flow cytometry. Data are represented as mean ± SEM of three technical replicates. Differences of expression (C and E), proliferation (F) and apoptosis (G) between groups were calculated by unpaired t test. *$p < 0.05$; **$p < 0.01$, ***$p < 0.001$. Also, see Figure S3.

Additionally, the IC_{50} values of imatinib for CML cells overexpressing *IRAIN* reduced from 1.891 ± 0.154 μM in K562/G01 Vector cells to 0.636 ± 0.037 μM in K562/G01 *IRAIN* cells (**$p = 0.0014 < 0.01$) and from 0.086 ± 0.004 μM in MEG-01 Vector cells to 0.071 ± 0.003 μM in MEG-01 *IRAIN* cells (*$p = 0.0247 < 0.05$, Figure 2E), indicating that overexpression of *IRAIN* was a suitable method of re-sensitizing CML cells to imatinib resistance.

Furthermore, knockdown of *IRAIN* significantly increased colony forming ability in K562 and MEG-01 cells at imatinib concentrations of 0, 0.1, 0.2, and 0.5 μM, respectively; and *IRAIN* upregulation significantly decreased the colony forming ability in K562/G01 cells at imatinib concentrations of 0, 1.0, 2.5, or 5.0 μM after 14 days of culturing (Figures 2F and S2G). The numbers of colonies increased from 161.0 ± 3.215, 124.7 ± 6.960, 68.67 ± 6.386, 5.667 ± 1.764 in K562 shNC cells at each concentration of imatinib, to 181.0 ± 2.082 164.7 ± 6.766, 114.0 ± 5.033, 32.67 ± 2.028 in K562 shIRAIN cells, and decreased from 391.3 ± 16.60, 325.3 ± 6.566, 112.7 ± 4.631, 50.00 ± 8.083 in K562/G01 Vector cells at each concentration of imatinib, to 304.7 ± 11.10, 93.67 ± 8.647, 5.00 ± 1.155, 1.667 ± 0.667 in K562/G01 *IRAIN* cells (Figure 2F). Similar trend was also observed in IRAIN- knocked-down or overexpressed MEG-01 cells (Figure S2G). These results indicate that *IRAIN* upregulation enable resensitization of CML cells to imatinib, resulting in reduction of colony-forming ability.

Imatinib resistance was overcome by *IRAIN*-downregulated CD44 expression in CML cell lines

The data above proved that the expression of *IRAIN* was the lowest in $CD34^+$ primary blasts and primary mononuclear cells (Figures 1A and 1B), resulting in imatinib resistance in CML (Figures 2 and S2). The $CD34^+$ primary CML blasts are usually considered leukemia stem cells; therefore, *IRAIN* may be involved in regulating LSC-related drug resistance. As shown in Figure 3A, whole-transcriptome RNA sequencing (RNA-seq) was performed on K562 Vector and K562 *IRAIN* cells to analyze the differential expression of genes related to LSCs. As a classical marker of stem cells and a key receptor in controlling drug resistance,[16,17,29] *CD44* was found to be downregulated in *IRAIN*-overexpressing K562 cells, based on the RNA-seq results (Figure 3A; Table S2). Furthermore, mononuclear cells were collected from seven newly diagnosed patients with CML. The expression of *IRAIN* was detected by the TaqMan probe qRT-PCR, and the cell surface CD44 receptor was detected using flow cytometry (Figure 3B). A reverse correlation was found between the expression of *IRAIN* and the CD44 protein, with a negative coefficient ($r = -0.75$) (*$p = 0.048 < 0.05$) (Figure 3B). The reverse correlation was observed in both CML cell line and CML mononuclear cells, indicating that *IRAIN* inhibited CD44 expression.

To determine whether the regulation of cell surface CD44 by *IRAIN* occurred at the transcriptional or translational level, *CD44* transcripts and CD44 protein were assayed in the CML cell lines K562 and MEG-01, which possessed *IRAIN* knockdown and overexpression, respectively. Using qRT-PCR, flow cytometry, and western blotting, *CD44* transcripts, cell surface CD44, and total CD44 protein expression were all upregulated in K562 siIRAIN and ME-G01 siIRAIN cells compared with those in control cells, K562 siNC and MEG-01 siNC (Figures 3C–3E). Conversely, when *IRAIN* was overexpressed in K562 and MEG-01 cells, they presented downregulated *CD44* transcripts and CD44 proteins (Figures 3C–3E).

Additionally, to exclude the possibility that the *BCR-ABL1* affects the regulation of *CD44*, the AML cell lines U937 and MV4-11, which carry no BCR-ABL1 fusion proteins (Figures S3A and S3B), were analyzed for the regulation of *CD44* by *IRAIN*. The detection showed that *CD44* transcripts and cell surface CD44 were downregulated in U937 *IRAIN* and MV4-11 *IRAIN* cells compared to those in U937 and MV4-11 Vector cells (Figures S3A and S3B). These data indicated that *CD44* was transcriptionally downregulated by *IRAIN* overexpression, and the regulation between *CD44* and *IRAIN* was not impacted by the *BCR-ABL1* oncoprotein in CML.

CD44 is commonly related to resistance to chemotherapeutic agents and impacts TKI resistance in CML.[16,19] To confirm imatinib resistance was caused by *IRAIN*-mediated *CD44* upregulation, *CD44* transcripts were knocked down by siRNA in K562 and MEG-01 siIRAIN cells. Efficiency of CD44 siRNA was confirmed using qRT-PCR and flow cytometry (Figures S3C and S3D). As shown in Figure 3F, cell proliferation increased in K562 siIRAIN cells compared to that in the control K562 cells transiently transfected with a negative control siRNA. The proliferation rates of K562 cells transfected with siRNA-mediated *IRAIN* and *CD44* were approximately equal to those of the control cells (Figure 3F). The proliferation rates of the MEG-01 cells transfected with siRNA-mediated *IRAIN*, *CD44*, or both showed similar trends as in the K562 cells (Figure S3E). Following the trends of the proliferation rates in the K562 and MEG-01 cells with the knockdown of *IRAIN* or *CD44*, the apoptosis rates induced by imatinib were decreased in K562 siIRAIN cells compared with those in siNC cells (Figure 3G). In contrast, the apoptosis levels in the K562 cells with siRNA-mediated *IRAIN* and *CD44* recovered to approximately equal levels to those of siNC cells (Figure 3G). A similar

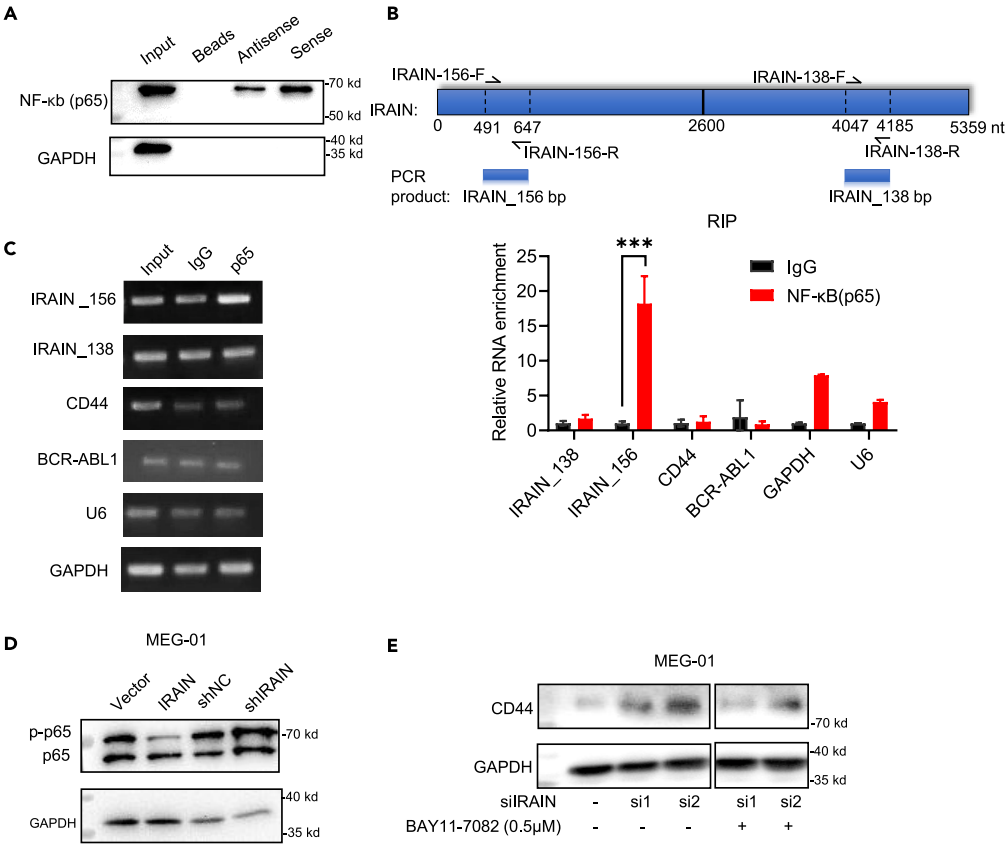

Figure 4. *IRAIN* binding to NF-κB reduced both p65 and phosphorylated p65, resulting in downregulation of CD44

(A) RNA pull-down assay was performed to detect the proteins binding to *in vitro* transcribed *IRAIN* sense and *IRAIN* antisense RNAs. The extracted proteins were resolved using western blotting.

(B and C) The primers of *IRAIN* used in qRT-PCR are shown schematically (upper panel of B). qRT-PCR (lower panel of B) and RT-PCR (C) were performed to detect the RNA fragments trapped by the p65 antibody in the RIP assay. IgG was used as a negative control of the p65 antibody. *GAPDH* and *U6* were used as reference genes of the cytoplasm and nucleus, respectively. Data are represented as mean ± SD of three technical replicates. Differences of expression between groups (B) were calculated by unpaired t test. *$p < 0.05$; **$p < 0.01$, ***$p < 0.001$.

(D) Western blotting was used for p65 and the phosphorylated p65 (p-p65) protein expression in MEG-01 cells when *IRAIN* was overexpressed and downregulated.

(E) MEG-01 cells transfected with two siRNAs against *IRAIN* (si1 or si2) were treated with either DMSO or NF-κB inhibitor Bay11-7082 for 48 h, and then CD44 levels were detected using western blotting. Also, see Figure S4.

result was observed in MEG-01 cells (Figure S3F). In summary, *IRAIN*-mediated downregulation of *CD44* contributes to overcoming imatinib resistance in CML.

IRAIN binding to NF-κB reduced both p65 and phosphorylated p65, resulting in downregulation of CD44

LncRNAs usually function in tumor development by interacting with one or more RNA-binding proteins (RBPs).[30] To explore the mechanism of *IRAIN*-regulated *CD44* expression, the candidate proteins interacting with *IRAIN* were predicted using catRAPID omics (v2.1), a web server used to predict the interaction propensities between proteins and RNAs by large-scale computation. As shown in Figure S4A, the NF-κB Repressing Factor (NKRF) ranked first out of the candidate RBP proteins, which can potentially bind to *IRAIN*. We then further analyzed the possibility of *IRAIN* interacting with NKRF and the five subunits of nuclear factor kappa B (NF-κB), including RELA/p65, NFKB1/p50, RelB, c-Rel, and NFKB2/p52, respectively, using the specialized predicting website (RPISeq: http://pridb.gdcb.iastate.edu/RPISeq/). The predictions showed that NF-κB subunit p65 had the highest correlation index with *IRAIN*, suggesting that p65 may have the most potential to interact with *IRAIN* (Figure S4B).

Previous studies have revealed that NF-κB can promote CD44 transcription in solid tumors.[31–33] We speculated that *IRAIN* may regulate CD44 by interacting with the NF-κB p65 in CML. Therefore, we constructed *IRAIN* expression plasmids tRSA-*IRAIN*-sense and tRSA-*IRAIN*-antisense to perform an RNA pull-down assay to capture the proteins that may bind to *IRAIN* in K562 cells. As expected, *IRAIN* pulled down the p65 protein, as confirmed by the p65 protein band on the western blot (Figure 4A). This finding verified the existence of an interaction

between *IRAIN* and p65 (Figure 4A). Conversely, an RNA-binding protein immunoprecipitation (RIP) assay was performed using a p65 antibody to trap the RNA fragments that bind to p65 in K562 cells. The data above indicated that p65 bound to the 5′ region of *IRAIN*, which was amplified by PCR using primer pairs spanning a 156 nucleotides (nt) region (named *IRAIN*_156) from 491 to 647 nt instead of binding to the 3′ region starting from 4047 to 4185 nt (named *IRAIN*_138) (Figures 4B and 4C).

In MEG-01 IRAIN cells, *IRAIN* overexpression was inversely correlated with the p65 and phosphorylated p65 protein levels (Figure 4D). Alternately, in K562 cells, the knockdown of *IRAIN* was related to an increased level of p65 (Figure S4C). However, the transcriptional level of RELA/p65 remained stable when *IRAIN* was overexpressed, indicating that p65 protein expression was not modulated at the transcription but at the translation level (Figure S4D). RELA/p65 activation upregulates CD44 in some solid cancers.[31–33] The CD44 transcription and protein levels were measured after inhibiting p65 expression using siRNA in MEG-01 cells (Figures S4E and S4F). The data showed that the transcription and translation levels of CD44 decreased after the knockdown of p65, indicating that NF-κB p65 expression could upregulate CD44 expression in CML cells. Nevertheless, when 0.5 μM NF-κB inhibitor, Bay11-7082, was added into MEG-01 siIRAIN cells, these cells were unable to upregulate CD44 expression, suggesting that the knockdown of *IRAIN* was unable to recover CD44 upregulation when Bay11-7082 specifically inhibited the p65 protein (Figures 4E, S4G, and S4H).

Collectively, *IRAIN* binding to the p65 protein was the basis for modulating CD44 in an NF-κB dependent manner.

IRAIN overexpression enhanced the sensitivity to imatinib in purified CD34$^+$ CML primary blasts *ex vivo*

IRAIN overexpression overcomes imatinib resistance in CML cell lines *in vitro*, and its effects need to be reconfirmed in CML primary blast cells *ex vivo*. The siRNA-mediated knockdown of *IRAIN* and lentivirus-mediated *IRAIN* overexpression were separately performed in sorted CD34$^+$ from two cases of CML primary blast cells and six cases of CML mononuclear cells before being exposed to imatinib. Imatinib-induced specific apoptosis levels[34] were analyzed using flow cytometry. The data showed that knocking down *IRAIN* decreased the sensitivity of CML cells to imatinib owing to a reduction in specific apoptosis levels (Figures 5A and 5B). Conversely, lentivirus-mediated *IRAIN* overexpression successfully increased *IRAIN* expression in six cases of CD34$^+$ sorted CML blast cells, as confirmed using qRT-PCR (Figure 5C), indicating that imatinib-induced specific apoptosis levels were significantly increased in five samples (Figure 5D). *IRAIN* overexpression decreased the viability of CD34$^+$ cells in a dose-dependent manner in all four patients with CML (Figure 5E). These data confirmed that *IRAIN* overexpression sensitizes CML primary blast cells to imatinib *ex vivo*.

Decitabine upregulated *IRAIN* and enhanced the sensitivity to imatinib in CML cell lines

As a tumor suppressor, *IRAIN* can serve as a therapeutic target independent of BCR-ABL1. *IRAIN* overexpression in CML cell lines or primary blasts can play a therapeutic role in overcoming imatinib resistance. Therefore, one solution to imatinib resistance is seeking an approved drug to increase *IRAIN* expression. A previous study revealed that the *IRAIN* promoter is hypermethylated in K562 cells.[24] Hence, we deduced that demethylation agents, such as DAC, can elevate *IRAIN* expression. DAC is commonly used as a hypomethylating agent to treat patients with myelodysplasia syndrome, elderly patients with acute myeloid leukemia, refractory/refractory acute myeloid leukemia, and the accelerated phase or blast phase of CML.[35–38] In the scenario of imatinib resistance, except for the induction of the BCR-ABL1 mutation, DAC can elevate the expression of *IRAIN*. It should be one of the key drugs for overcoming imatinib resistance in CML.

To test the effect of DAC on *IRAIN* in CML cells, the IC_{50} values of DAC used for K562 and MEG-01 cells were determined by their IC_{50} curves (Figures S6A and S6B). The K562 cells were treated with 10 μM of DAC for 48 h, and *IRAIN* expression was significantly increased compared with that in the control cells (Figure 6A). Moreover, we verified *IRAIN* levels in BMMNCs from two patients with TKI-resistant CML before and after receiving DAC (15 mg/m^2) intravenously for five consecutive days.[37] As expected, *IRAIN* levels were increased after DAC treatment (Figure 6B). We then treated K562 and MEG-01 cells with imatinib and DAC separately and together. We observed that combining imatinib with DAC accelerated cell apoptosis (Figure 6C) and inhibited cell proliferation (Figure 6D) compared to single-drug therapy. To further confirm whether DAC acts on CML cells in an *IRAIN*-dependent manner, we knocked down *IRAIN* using siRNA in DAC-treated K562/G01 and MEG-01 cells. We found that the apoptosis levels in *IRAIN*-knocked-down cells decreased compared to those in the negative controls, indicating that *IRAIN* knockdown attenuated the apoptotic function of DAC in CML cell lines (Figure 6E). Based on these findings, we concluded that DAC sensitizes CML cells to imatinib via *IRAIN* upregulation.

DISCUSSION

Presently, two major aims of CML therapy are the prolongation of overall survival and achievement of TKI discontinuation in patients who have received treatment for a minimum of 2–3 years and reached a durable deep molecular response (DMR) of MR 4 or MR 4.5 (*BCR-ABL1* transcripts with a 4-log reduction or a 4.5-log reduction from a standardized baseline on the IS respectively,[8] for over two years).[6,9,10] Therefore, a deeper and faster molecular response on starting TKIs is critical to ensure a promising long-term outcome. For instance, patients with CML who reached response milestones of ≤10% *BCR-ABL1* transcripts by three months, ≤1% by six months, or ≤0.1% by 12 months on the IS[8] have high survival probabilities.[6,7] However, patients with CML gained an MR of 4.5 when treated with dasatinib or imatinib at 42% or 33% after 5-year follow-up, respectively.[39] This data suggests that over half of patients with CML could not achieve an optimal DMR at indicated time points. The main causes were primary TKI resistance, which failed to achieve an optimal response to primary therapy, and secondary TKI resistance, which relapsed after achieving an initial response.[40] The incidence of primary and secondary resistance to frontline TKI imatinib is 10% and 30%, respectively.[41] Hence, the resolution of TKI resistance should lead to a promising outcome in patients with CML.

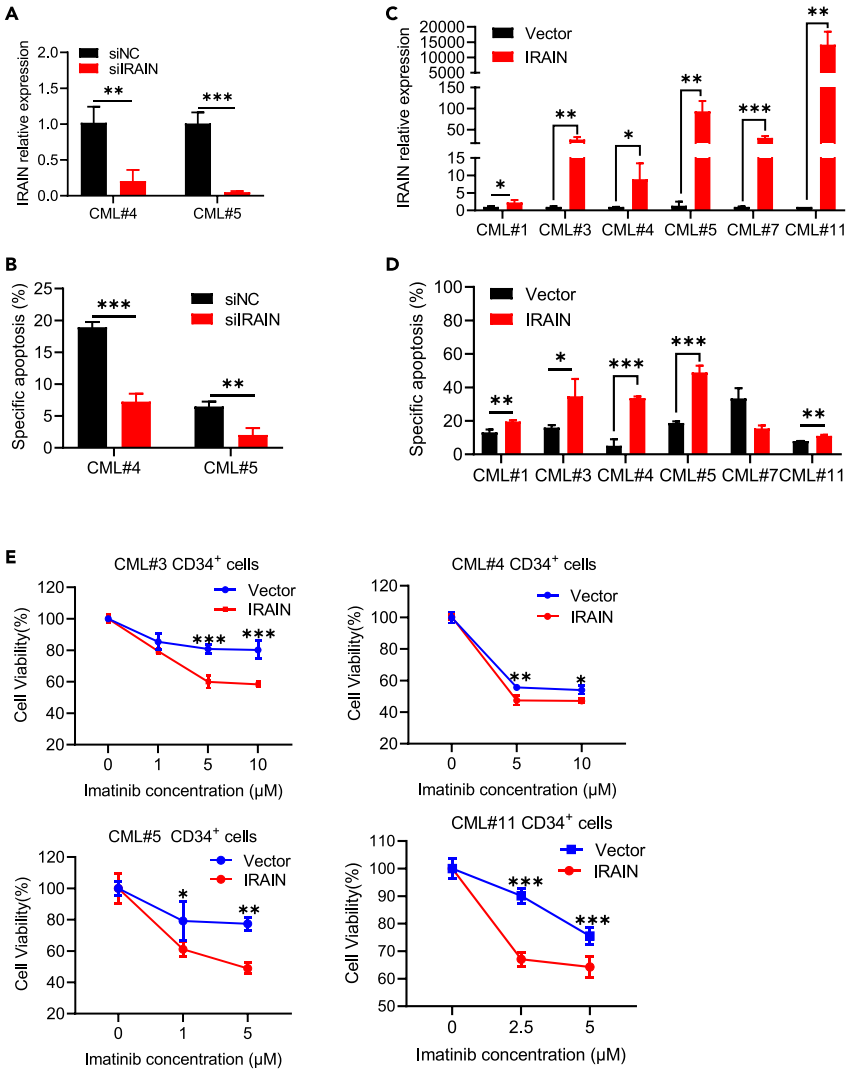

Figure 5. *IRAIN* overexpression enhanced the sensitivity to imatinib in purified CD34⁺ CML primary blasts *ex vivo*

(A and B) Bone marrow mononuclear cells (BMMNCs) from two patients with CML (CML #4 and CML #5) were transfected with siRNA against *IRAIN* (siIRAIN) or the negative control siRNA (siNC). (A) The levels of *IRAIN* were detected using qRT-PCR after 48 h of transfection, with *GAPDH* used as a reference gene. Data are represented as mean ± SD of three technical replicates. (B) The transfected cells were treated with imatinib for 48 h, and imatinib-induced specific apoptosis levels were analyzed using flow cytometry through the Annexin V/PI dual staining. Data are represented as mean ± SEM of three biological replicates.
(C–E) RNA levels of *IRAIN* (C) were detected using qRT-PCR in BMMNCs obtained from patients with CML and transfected with the lentivirus expressing either *IRAIN* or the vector for 48 h. Data are represented as mean ± SD of three technical replicates. These transfected cells were treated with imatinib for another 48 h, and imatinib-induced specific apoptosis (D) was analyzed using flow cytometry through Annexin V/PI dual staining, and cell viabilities were detected using CCK8 assay. Data are represented as mean ± SEM of three biological replicates. Differences between groups (A, B, C, D and E) were calculated by unpaired Student's t test; *$p < 0.05$, **$p < 0.01$, ***$p < 0.001$.

Whether primary or secondary, TKI resistance can be attributed to either a BCR-ABL1 kinase-dependent or -independent mechanism or both.[11] Primary resistance is mainly caused by BCR-ABL1 kinase-independent mechanisms, including epigenetic reprogramming, activation of signaling pathways downstream of *BCR-ABL1*, and microenvironmental factors such as *CD44* and *CXCR4*.[12,42–45] Secondary imatinib resistance is usually related to *BCR-ABL1* kinase domain mutations, which happens in at least 60% of such patients.[11] The rest are caused by the activation of 'bypass tracks', which serve as compensatory signaling loops or histological transformations.[46] More than 100 BCR-ABL1 kinase domain mutations have been reported.[47] Most mutations compromise imatinib binding to BCR-ABL1 kinase, decreasing sensitivity.[11,48] It can be resolved by switching to on-target second and third generations of TKIs, seeking an off-target therapeutic agent, or combining both. Off-targets are usually defined as genes and proteins regulated in CML compared with those in normal stem cells, and their expression and activity are not normalized by kinase inhibitors.[42] LSCs are one of the leading causes of primary or secondary resistance to CML. BCR-ABL1 kinase activity can be fully inhibited within the most primitive CML stem and progenitor cells without the induction of apoptosis.[14,49] Individuals

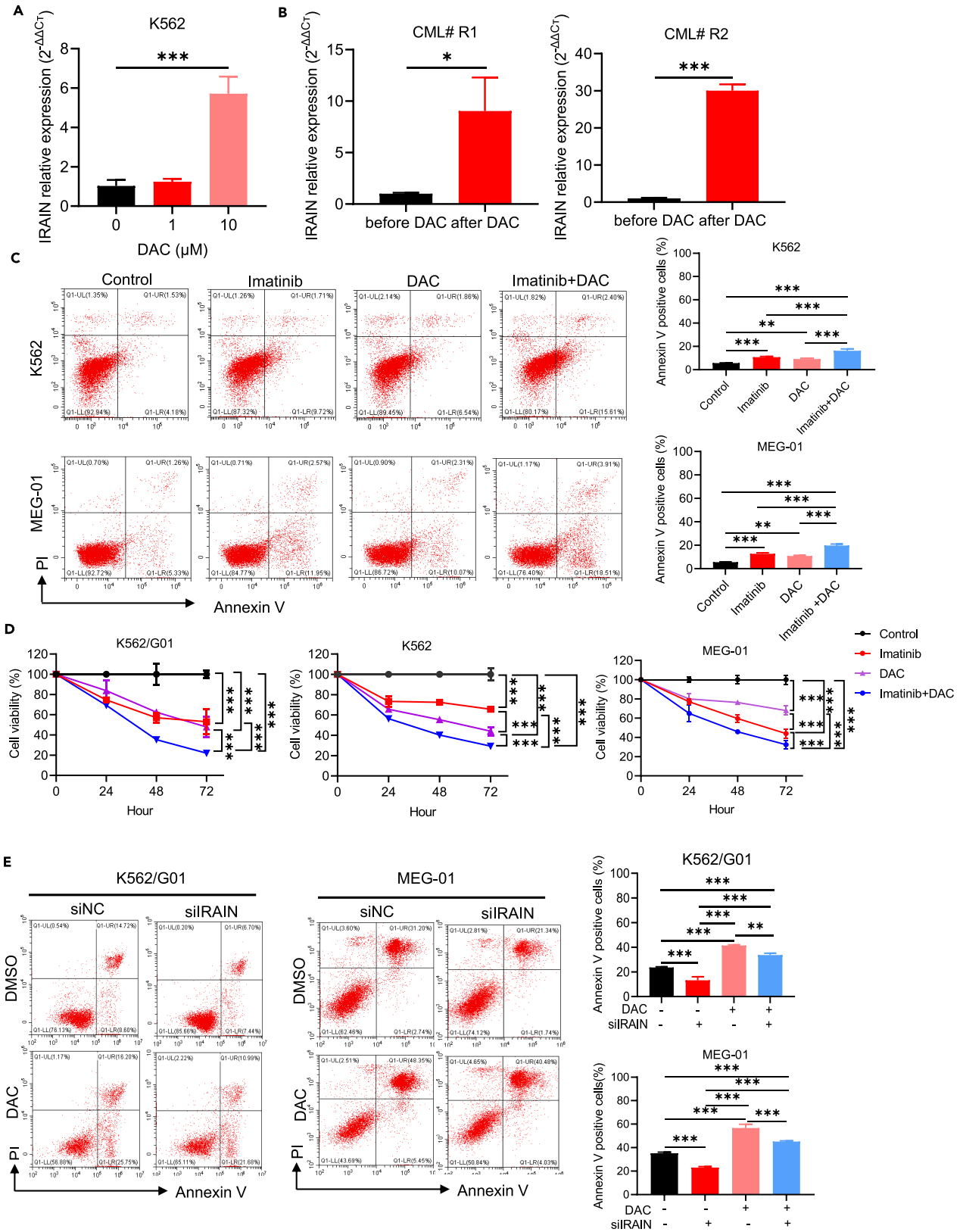
A
K562
IRAIN relative expression ($2^{-\Delta\Delta C_T}$)
DAC (μM)
B
CML# R1
CML# R2
before DAC after DAC
C
Control
Imatinib
DAC
Imatinib+DAC
K562
MEG-01
PI
Annexin V
Annexin V positive cells (%)
Imatinib +DAC
D
K562/G01
Cell viability (%)
Hour
Control
Imatinib
DAC
Imatinib+DAC
E
siNC
siIRAIN
DMSO
DAC
Annexin V positive cells(%)

Figure 6. Decitabine upregulated *IRAIN* and enhanced the sensitivity to imatinib in CML cell lines

(A) qRT-PCR was used to detect the relative expression levels of *IRAIN* in cells cultured with DAC for 48 h. *GAPDH* was used as a reference gene. Data are represented as mean ± SD of three technical replicates.

(B) Two TKI-resistant CML patients received DAC intravenously for five days, and *IRAIN* expression levels of the BMMNCs of these patients before and after receiving DAC treatment were measured by qRT-PCR. Data are represented as mean ± SD of three technical replicates.

(C and D) The K562 and MEG-01 cells were exposed to imatinib (0.1 μM for both K562 and MEG-01 cells) or DAC (10 μM for K562, 1.0 μM for MEG-01) or both drugs for up to 72 h. Apoptosis levels (C) were detected using flow cytometry after 48 h of drug exposure. Data are presented as mean ± SEM of three biological replicates. The cell viabilities (D) of K562, K562/G01 (2.5 μM of imatinib, 10 μM of DAC), and MEG-01 cells were determined by the CCK8 method when cells were exposed to drugs for 0, 24, 48, and 72 h. Data are presented as mean ± SEM of three biological replicates.

(E) The K562/G01 and MEG-01 cells were pretreated with DAC (10 μM for K562/G01, 1.0 μM for MEG-01) or DMSO as a control for 48 h and then transfected with siRNA against *IRAIN* (siIRAIN). Apoptosis levels were detected by flow cytometry at 48 h post-transfection. Data are presented as mean ± SEM of three biological replicates. Differences of expression between groups (A and B) were calculated by unpaired t test, and differences of apoptosis (C and E) and cell viability (D) were calculated by ANOVA test. $*p < 0.05$; $**p < 0.01$, $***p < 0.001$.

with undetectable *BCR-ABL1* transcripts by PCR may harbor as many as 6.5×10^6 residual leukemia cells.[50] Thus, leukemia-specific but off-target therapies combined with TKIs may form a dual therapy combination to eradicate CML. For instance, Zhou et al. described that the combination of targeting WNT/β-catenin and BCR-ABL1 could induce apoptosis in CML blasts and progenitors.[34] Scott et al. reported that the combined inhibition of epigenetic regulators *EZH2* or *SIRT1* and *BCR-ABL1* resulted in synergistic elimination of CML stem cells.[51]

In the present study, *IRAIN* was constitutively downregulated in BMMNCs from patients with CML compared with that in healthy controls, and *IRAIN* was related to TKI resistance because of its lower expression in $CD34^+$ cells than in $CD34^-$ cells and in resistant K562/G01 cells than in sensitive K562 cells (Figure 1). The siRNA-mediated knockdown of *IRAIN* in sorted $CD34^+$ and other CML cell lines decreased their sensitivity to imatinib, as evidenced by reduced apoptosis and increased cell viability. Conversely, the overexpression of *IRAIN* in these cells increased their sensitivity to imatinib, as demonstrated by the increased apoptosis levels and decreased cell viability (Figure 2). These results indicate that the upregulation of *IRAIN* can overcome imatinib resistance; therefore, *IRAIN* can serve as a therapeutic target. As shown in Figure 1, siRNA-mediated knockdown of *BCR-ABL1* had no impact on *IRAIN*. Consequently, it was a leukemia-specific but BCR-ABL1 kinase-independent target.

LSCs reside in the bone marrow microenvironment, which provides a sanctuary for subpopulations of leukemic cells to evade chemotherapy-induced death and allow the acquisition of a drug-resistant phenotype.[14,52] The CD44, a cell surface receptor, maintains LSCs to survive in the microenvironment. Thus, CD44 expression may help eradicate LSCs.[16,52–54] In CML, the BCR-ABL1-upregulated CD44 can be abolished by the BCR-ABL1 inhibitor imatinib.[16] Furthermore, *IRAIN* downregulated CD44 expression in CML (Figure 3), indicating CD44 can serve as a dual therapeutic target by both upregulated *IRAIN* and imatinib. The present study investigated the regulatory mechanism of *CD44* in *IRAIN*. As shown in Figure 4, there is a specific binding between *IRAIN* and the NF-κB subunit p65. This interaction subsequently reduces the p65 protein and phosphorylated p65 levels, reducing CD44 expression at transcription and translation levels. Therefore, CD44 was regulated by *IRAIN* via the NF-κB pathway, and the relationship between NF-κB and CD44 in hematological disorders has been disclosed. The NF-κB pathway is also activated by BCR-ABL to maintain CML.[55,56] Hence, we considered that RelA/p65 in the NF-κB pathway is the merged pivot to regulated CD44 in CML, which paves the basis for dual therapy through regulating *IRAIN* and inhibiting BCR-ABL1 kinase activity. Furthermore, we also demonstrated that NF-κB positively regulates CD44 and that inhibition of NF-κB with its inhibitor Bay11-7082 or by siRNA-mediated knockdown of p65 decreased CD44 mRNA and protein levels. These results suggest that NF-κB can be a therapeutical target to overcome TKI resistance.

The upregulation of *IRAIN* can overcome imatinib resistance (Figure 2). As shown in Figure 6, the approved hypomethylation drug decitabine successfully upregulated *IRAIN* expression in both CML cell lines and patients with CML, as the *IRAIN* promoter is hypermethylated in CML cells.[24] Furthermore, we confirmed a synergistic effect with decitabine combined with imatinib in CML cells. Therefore, the combination of decitabine and imatinib is superior to TKI alone, and it should be considered an optimal treatment, which has also been reported elsewhere for patients with CML in the myeloid blast phase.[37,57] However, decitabine is a multitarget drug which can not only upregulate *IRAIN* but also change the methylation levels of other genes.[58,59] Approaches for increasing RNA payloads, such as self-amplifying RNAs, are still in need of further research.

Previously, the involvement of *IRAIN* with drug resistance has been described in gliomas via repressing the IGF-1R-PI3K-NF-κB axis.[28] The effects of *IRAIN* in carcinogenesis have been described in breast cancer, non-M3 AML, and pancreatic cancer.[25,27,60] In this study, we confirmed that the cancer stem cell marker CD44, associated with resistance to chemo- and radiotherapies,[61] can be downregulated by upregulating *IRAIN* independent of *BCR-ABL1* in CML. We deduce that the upregulation of *IRAIN* should overcome drug resistance in solid tumors and other leukemias. For instance, *IRAIN* overexpression decreased CD44 mRNA and protein levels in the AML cell lines MV4-11 and U937 (Figure S3).

In conclusion, *IRAIN* binding to p65 reduced p65 and phosphorylated p65 levels, decreasing CD44 levels and thus overcoming imatinib resistance independent of *BCR-ABL1*. Therefore, decitabine, which upregulates *IRAIN*, and imatinib form a dual therapy strategy for CML.

Limitations of the study

This study has some limitations and unsolved areas. Through RNA pull-down and RIP, we identified NF-κB p65 as an RNA-binding protein in *IRAIN*. We confirmed that the *IRAIN* (upper segment) binds to NF-κB p65 physically. However, the responsible amino acid on p65 and whether this segment of *IRAIN* is the functional segment in CML need further exploration. In addition, p65 and phosphorylated p65 levels decreased due to *IRAIN* binding; however, how *IRAIN* downregulates or inhibits the phosphorylation of the proteins needs to be studied more in-depth.

STAR★METHODS

Detailed methods are provided in the online version of this paper and include the following:

SUPPLEMENTAL INFORMATION

Supplemental information can be found online at https://doi.org/10.1016/j.isci.2024.109851.

ACKNOWLEDGMENTS

Thanks to Dr. Jingnan Sun (Jilin University, Changchun 130061, China) for sharing plasmids *IRAIN*-constructed pCDH-CMV-MCS-EF1-CopGFP-T2A-Puro and empty vector. Thanks to Professor Haixin Lei (Dalian Medical University, Dalian 116027, China) for his instruction on writing manuscript. Thanks to Yuchao Hao as our colleagues for technical assistance.

This work was mainly funded by the Central Guidance on Local Science and Technology Development Fund of Liaoning Province (2023JH6/100100019 to J.-S.Y.), and partially funded by Science and Technology Innovation Leading Talent Program of Liaoning Province (XLYC1902036 to J.-S.Y.), Basic Research on the Application of Dalian Innovation Fund (2019J12SN56 to J.-S.Y.), Key R & D projects in Liaoning Province (2019JH8/10300027 to J.-S.Y.), and Key Project of the Educational Department of Liaoning Province (LZ2020003 to J.-S.Y).

AUTHOR CONTRIBUTIONS

Conceptualization and design, J.Y., X.Z., and F.X.; methodology, X.W., Y.H., Y.L., J.Z., X.Z., and D.H.; software, X.W. and Y.H.; formal analysis, X.W.; investigation, X.W. and Y.L.; validation, J.Y. and F.X.; resources, X.W., D.H., Z.Z., and D.Z.; writing original draft, X.W. and M.A.H.; writing, review and editing, J.Y., X.Z., and F.X.; visualization, X.W., Y.H., and F.X.; supervision, J.Y., X.Z., and F.X.; project administration, J.Y.; funding acquisition, J.Y.

DECLARATION OF INTERESTS

The authors declare no competing interests.

Received: November 15, 2023
Revised: March 8, 2024
Accepted: April 26, 2024
Published: April 30, 2024

REFERENCES

1. Jabbour, E., and Kantarjian, H. (2018). Chronic myeloid leukemia: 2018 update on diagnosis, therapy and monitoring. Am. J. Hematol. *93*, 442–459. https://doi.org/10.1002/ajh.25011.
2. Dagogo-Jack, I., and Shaw, A.T. (2018). Tumour heterogeneity and resistance to cancer therapies. Nat. Rev. Clin. Oncol. *15*, 81–94. https://doi.org/10.1038/nrclinonc.2017.166.
3. Jiao, Q., Bi, L., Ren, Y., Song, S., Wang, Q., and Wang, Y.S. (2018). Advances in studies of tyrosine kinase inhibitors and their acquired resistance. Mol. Cancer *17*, 36. https://doi.org/10.1186/s12943-018-0801-5.
4. Druker, B.J., Tamura, S., Buchdunger, E., Ohno, S., Segal, G.M., Fanning, S., Zimmermann, J., and Lydon, N.B. (1996). Effects of a selective inhibitor of the Abl tyrosine kinase on the growth of Bcr-Abl positive cells. Nat. Med. *2*, 561–566. https://doi.org/10.1038/nm0596-561.
5. Druker, B.J., Guilhot, F., O'Brien, S.G., Gathmann, I., Kantarjian, H., Gattermann, N., Deininger, M.W.N., Silver, R.T., Goldman, J.M., Stone, R.M., et al. (2006). Five-year follow-up of patients receiving imatinib for chronic myeloid leukemia. N. Engl. J. Med. *355*, 2408–2417. https://doi.org/10.1056/NEJMoa062867.
6. Soverini, S., Bassan, R., and Lion, T. (2019). Treatment and monitoring of Philadelphia chromosome-positive leukemia patients: recent advances and remaining challenges. J. Hematol. Oncol. *12*, 39. https://doi.org/10.1186/s13045-019-0729-2.
7. Hehlmann, R., Lauseker, M., Saußele, S., Pfirrmann, M., Krause, S., Kolb, H.J., Neubauer, A., Hossfeld, D.K., Nerl, C., Gratwohl, A., et al. (2017). Assessment of imatinib as first-line treatment of chronic myeloid leukemia: 10-year survival results of the randomized CML study IV and impact of non-CML determinants. Leukemia *31*, 2398–2406. https://doi.org/10.1038/leu.2017.253.
8. Cross, N.C.P., White, H.E., Müller, M.C., Saglio, G., and Hochhaus, A. (2012). Standardized definitions of molecular response in chronic myeloid leukemia. Leukemia *26*, 2172–2175. https://doi.org/10.1038/leu.2012.104.
9. Jabbour, E., and Kantarjian, H. (2022). Chronic myeloid leukemia: 2022 update on diagnosis, therapy, and monitoring. Am. J. Hematol. *97*, 1236–1256. https://doi.org/10.1002/ajh.26642.
10. Pavlovsky, C., Abello Polo, V., Pagnano, K., Varela, A.I., Agudelo, C., Bianchini, M., Boquimpani, C., Centrone, R., Conchon, M., Delgado, N., et al. (2021). Treatment-free remission in patients with chronic myeloid leukemia: recommendations of the LALNET expert panel. Blood Adv. *5*, 4855–4863. https://doi.org/10.1182/bloodadvances.2020003235.
11. Braun, T.P., Eide, C.A., and Druker, B.J. (2020). Response and Resistance to BCR-ABL1-Targeted Therapies. Cancer Cell *37*, 530–542. https://doi.org/10.1016/j.ccell.2020.03.006.
12. Hehlmann, R. (2020). Chronic Myeloid Leukemia in 2020. Hemasphere *4*, e468. https://doi.org/10.1097/HS9.0000000000000468.
13. Kantarjian, H.M., Shan, J., Jones, D., O'Brien, S., Rios, M.B., Jabbour, E., and Cortes, J. (2009). Significance of increasing levels of minimal residual disease in patients with Philadelphia chromosome-positive chronic myelogenous leukemia in complete cytogenetic response. J. Clin. Oncol. *27*, 3659–3663. https://doi.org/10.1200/JCO.2008.18.6999.
14. Corbin, A.S., Agarwal, A., Loriaux, M., Cortes, J., Deininger, M.W., and Druker, B.J. (2011). Human chronic myeloid leukemia stem cells are insensitive to imatinib despite inhibition of BCR-ABL activity. J. Clin. Invest. *121*, 396–409. https://doi.org/10.1172/JCI35721.
15. Ito, K., and Ito, K. (2021). Leukemia Stem Cells as a Potential Target to Achieve Therapy-Free Remission in Chronic Myeloid Leukemia. Cancers *13*, 5822. https://doi.org/10.3390/cancers13225822.
16. Godavarthy, P.S., Kumar, R., Herkt, S.C., Pereira, R.S., Hayduk, N., Weissenberger, E.S., Aggoune, D., Manavski, Y., Lucas, T., Pan, K.T., et al. (2020). The vascular bone marrow niche influences outcome in chronic myeloid leukemia via the E-selectin - SCL/TAL1 - CD44 axis. Haematologica *105*, 136–147. https://doi.org/10.3324/haematol.2018.212365.
17. Yu, X., Munoz-Sagredo, L., Streule, K., Muschong, P., Bayer, E., Walter, R.J., Gutjahr, J.C., Greil, R., Concha, M.L., Müller-Tidow, C., et al. (2021). CD44 loss of function sensitizes AML cells to the BCL-2 inhibitor venetoclax by decreasing CXCL12-driven survival cues. Blood *138*, 1067–1080. https://doi.org/10.1182/blood.2020006343.
18. Hu, Y., and Li, S. (2016). Survival regulation of leukemia stem cells. Cell. Mol. Life Sci. *73*, 1039–1050. https://doi.org/10.1007/s00018-015-2108-7.
19. Krause, D.S., Lazarides, K., von Andrian, U.H., and Van Etten, R.A. (2006). Requirement for CD44 in homing and engraftment of BCR-ABL-expressing leukemic stem cells. Nat. Med. *12*, 1175–1180. https://doi.org/10.1038/nm1489.
20. Lompardia, S., Diaz, M., Pibuel, M., Papademetrio, D., Poodts, D., Mihalez, C., Alvarez, E., and Hajos, S. (2019). Hyaluronan abrogates imatinib-induced senescence in chronic myeloid leukemia cell lines. Sci. Rep. *9*, 10930. https://doi.org/10.1038/s41598-019-47248-8.
21. Wang, Y., Hu, S.B., Wang, M.R., Yao, R.W., Wu, D., Yang, L., and Chen, L.L. (2018). Genome-wide screening of NEAT1 regulators reveals cross-regulation between paraspeckles and mitochondria. Nat. Cell Biol. *20*, 1145–1158. https://doi.org/10.1038/s41556-018-0204-2.
22. Li, Z.Y., Yang, L., Liu, X.J., Wang, X.Z., Pan, Y.X., and Luo, J.M. (2018). The Long Noncoding RNA MEG3 and its Target miR-147 Regulate JAK/STAT Pathway in Advanced Chronic Myeloid Leukemia. EBioMedicine *34*, 61–75. https://doi.org/10.1016/j.ebiom.2018.07.013.
23. Li, Z., Yang, L., Liu, X., Nie, Z., and Luo, J. (2018). Long noncoding RNA MEG3 inhibits proliferation of chronic myeloid leukemia cells by sponging microRNA21. Biomed. Pharmacother. *104*, 181–192. https://doi.org/10.1016/j.biopha.2018.05.047.
24. Sun, J., Li, W., Sun, Y., Yu, D., Wen, X., Wang, H., Cui, J., Wang, G., Hoffman, A.R., and Hu, J.F. (2014). A novel antisense long noncoding RNA within the IGF1R gene locus is imprinted in hematopoietic malignancies. Nucleic Acids Res. *42*, 9588–9601. https://doi.org/10.1093/nar/gku549.
25. Pian, L., Wen, X., Kang, L., Li, Z., Nie, Y., Du, Z., Yu, D., Zhou, L., Jia, L., Chen, N., et al. (2018). Targeting the IGF1R Pathway in Breast Cancer Using Antisense lncRNA-Mediated Promoter cis Competition. Mol. Ther. Nucleic Acids *12*, 105–117. https://doi.org/10.1016/j.omtn.2018.04.013.
26. Guo, A., Fang, G., Lin, Z., Zheng, S., Zhuang, Z., Lin, R., and Lin, Y. (2022). Overexpression of lncRNA IRAIN restrains the progression and Temozolomide resistance of glioma via repressing IGF-1R-PI3K-NF-kappaB signaling pathway. Histol. Histopathol. *37*, 543–554. https://doi.org/10.14670/HH-18-425.
27. Lian, Y., Wang, J., Feng, J., Ding, J., Ma, Z., Li, J., Peng, P., De, W., and Wang, K. (2016). Long non-coding RNA IRAIN suppresses apoptosis and promotes proliferation by binding to LSD1 and EZH2 in pancreatic cancer. Tumour Biol. *37*, 14929–14937. https://doi.org/10.1007/s13277-016-5380-8.
28. Guo, A., Fang, G., Lin, Z., Zheng, S., Zhuang, Z., Lin, R., and Lin, Y. (2022). Overexpression of lncRNA IRAIN restrains the progression and Temozolomide resistance of glioma via repressing IGF-1R-PI3K-NF-κB signaling pathway. Histol. Histopathol. *37*, 543–554. https://doi.org/10.14670/hh-18-425.
29. Li, W., Ji, M., Lu, F., Pang, Y., Dong, X., Zhang, J., Li, P., Ye, J., Zang, S., Ma, D., and Ji, C. (2018). Novel AF1q/MLLT11 favorably affects imatinib resistance and cell survival in chronic myeloid leukemia. Cell Death Dis. *9*, 855. https://doi.org/10.1038/s41419-018-0900-7.
30. Ferre, F., Colantoni, A., and Helmer-Citterich, M. (2016). Revealing protein-lncRNA interaction. Brief. Bioinform. *17*, 106–116. https://doi.org/10.1093/bib/bbv031.
31. Smith, S.M., Lyu, Y.L., and Cai, L. (2014). NF-kappaB affects proliferation and invasiveness of breast cancer cells by regulating CD44 expression. PLoS One *9*, e106966. https://doi.org/10.1371/journal.pone.0106966.
32. Zhang, M., Wang, L., Yue, Y., Zhang, L., Liu, T., Jing, M., Liang, X., Ma, M., Xu, S., Wang, K., et al. (2021). ITPR3 facilitates tumor growth, metastasis and stemness by inducing the NF-kB/CD44 pathway in urinary bladder carcinoma. J. Exp. Clin. Cancer Res. *40*, 65. https://doi.org/10.1186/s13046-021-01866-1.
33. Haria, D., Trinh, B.Q., Ko, S.Y., Barengo, N., Liu, J., and Naora, H. (2015). The homeoprotein DLX4 stimulates NF-kappaB activation and CD44-mediated tumor-mesothelial cell interactions in ovarian cancer. Am. J. Pathol. *185*, 2298–2308. https://doi.org/10.1016/j.ajpath.2015.04.004.
34. Zhou, H., Mak, P.Y., Mu, H., Mak, D.H., Zeng, Z., Cortes, J., Liu, Q., Andreeff, M., and Carter, B.Z. (2017). Combined inhibition of beta-catenin and Bcr-Abl synergistically targets tyrosine kinase inhibitor-resistant blast crisis chronic myeloid leukemia blasts and progenitors *in vitro* and *in vivo*. Leukemia *31*, 2065–2074. https://doi.org/10.1038/leu.2017.87.
35. Welch, J.S., Petti, A.A., Miller, C.A., Fronick, C.C., O'Laughlin, M., Fulton, R.S., Wilson, R.K., Baty, J.D., Duncavage, E.J., Tandon, B., et al. (2016). TP53 and Decitabine in Acute Myeloid Leukemia and Myelodysplastic Syndromes. N. Engl. J. Med. *375*, 2023–2036. https://doi.org/10.1056/NEJMoa1605949.
36. Santini, V. (2019). How I treat MDS after hypomethylating agent failure. Blood *133*,

521–529. https://doi.org/10.1182/blood-2018-03-785915.
37. Oki, Y., Kantarjian, H.M., Gharibyan, V., Jones, D., O'Brien, S., Verstovsek, S., Cortes, J., Morris, G.M., Garcia-Manero, G., and Issa, J.P.J. (2007). Phase II study of low-dose decitabine in combination with imatinib mesylate in patients with accelerated or myeloid blastic phase of chronic myelogenous leukemia. Cancer *109*, 899–906. https://doi.org/10.1002/cncr.22470.
38. Jiang, L.C., and Luo, J.M. (2017). Role and mechanism of decitabine combined with tyrosine kinase inhibitors in advanced chronic myeloid leukemia cells. Oncol. Lett. *14*, 1295–1302. https://doi.org/10.3892/ol.2017.6318.
39. Cortes, J.E., Saglio, G., Kantarjian, H.M., Baccarani, M., Mayer, J., Boqué, C., Shah, N.P., Chuah, C., Casanova, L., Bradley-Garelik, B., et al. (2016). Final 5-Year Study Results of DASISION: The Dasatinib Versus Imatinib Study in Treatment-Naïve Chronic Myeloid Leukemia Patients Trial. J. Clin. Oncol. *34*, 2333–2340. https://doi.org/10.1200/jco.2015.64.8899.
40. Bixby, D., and Talpaz, M. (2011). Seeking the causes and solutions to imatinib-resistance in chronic myeloid leukemia. Leukemia *25*, 7–22. https://doi.org/10.1038/leu.2010.238.
41. Zhang, W.W., Cortes, J.E., Yao, H., Zhang, L., Reddy, N.G., Jabbour, E., Kantarjian, H.M., and Jones, D. (2009). Predictors of primary imatinib resistance in chronic myelogenous leukemia are distinct from those in secondary imatinib resistance. J. Clin. Oncol. *27*, 3642–3649. https://doi.org/10.1200/jco.2008.19.4076.
42. Holyoake, T.L., and Helgason, G.V. (2015). Do we need more drugs for chronic myeloid leukemia? Immunol. Rev. *263*, 106–123. https://doi.org/10.1111/imr.12234.
43. Vicente-Duenas, C., Gonzalez-Herrero, I., Sehgal, L., Garcia-Ramirez, I., Rodriguez-Hernandez, G., Pintado, B., Blanco, O., Criado, F.J.G., Cenador, M.B.G., Green, M.R., et al. (2019). Dnmt1 links BCR-ABLp210 to epigenetic tumor stem cell priming in myeloid leukemia. Leukemia *33*, 249–278. https://doi.org/10.1038/s41375-018-0192-z.
44. Ko, T.K., Javed, A., Lee, K.L., Pathiraja, T.N., Liu, X., Malik, S., Soh, S.X., Heng, X.T., Takahashi, N., Tan, J.H.J., et al. (2020). An integrative model of pathway convergence in genetically heterogeneous blast crisis chronic myeloid leukemia. Blood *135*, 2337–2353. https://doi.org/10.1182/blood.2020004834.
45. Shah, N.P., Nicoll, J.M., Nagar, B., Gorre, M.E., Paquette, R.L., Kuriyan, J., and Sawyers, C.L. (2002). Multiple BCR-ABL kinase domain mutations confer polyclonal resistance to the tyrosine kinase inhibitor imatinib (STI571) in chronic phase and blast crisis chronic myeloid leukemia. Cancer Cell *2*, 117–125. https://doi.org/10.1016/s1535-6108(02)00096-x.
46. Lovly, C.M., and Shaw, A.T. (2014). Molecular pathways: resistance to kinase inhibitors and implications for therapeutic strategies. Clin. Cancer Res. *20*, 2249–2256. https://doi.org/10.1158/1078-0432.Ccr-13-1610.
47. Mughal, T.I., Radich, J.P., Deininger, M.W., Apperley, J.F., Hughes, T.P., Harrison, C.J., Gambacorti-Passerini, C., Saglio, G., Cortes, J., and Daley, G.Q. (2016). Chronic myeloid leukemia: reminiscences and dreams. Haematologica *101*, 541–558. https://doi.org/10.3324/haematol.2015.139337.
48. Corbin, A.S., La Rosée, P., Stoffregen, E.P., Druker, B.J., and Deininger, M.W. (2003). Several Bcr-Abl kinase domain mutants associated with imatinib mesylate resistance remain sensitive to imatinib. Blood *101*, 4611–4614. https://doi.org/10.1182/blood-2002-12-3659.
49. Hamilton, A., Helgason, G.V., Schemionek, M., Zhang, B., Myssina, S., Allan, E.K., Nicolini, F.E., Müller-Tidow, C., Bhatia, R., Brunton, V.G., et al. (2012). Chronic myeloid leukemia stem cells are not dependent on Bcr-Abl kinase activity for their survival. Blood *119*, 1501–1510. https://doi.org/10.1182/blood-2010-12-326843.
50. Sender, R., Fuchs, S., and Milo, R. (2016). Revised Estimates for the Number of Human and Bacteria Cells in the Body. PLoS Biol. *14*, e1002533. https://doi.org/10.1371/journal.pbio.1002533.
51. Scott, M.T., Korfi, K., Saffrey, P., Hopcroft, L.E.M., Kinstrie, R., Pellicano, F., Guenther, C., Gallipoli, P., Cruz, M., Dunn, K., et al. (2016). Epigenetic Reprogramming Sensitizes CML Stem Cells to Combined EZH2 and Tyrosine Kinase Inhibition. Cancer Discov. *6*, 1248–1257. https://doi.org/10.1158/2159-8290.CD-16-0263.
52. Konopleva, M., Tabe, Y., Zeng, Z., and Andreeff, M. (2009). Therapeutic targeting of microenvironmental interactions in leukemia: mechanisms and approaches. Drug Resist. Updates *12*, 103–113. https://doi.org/10.1016/j.drup.2009.06.001.
53. Lim, J.R., Mouawad, J., Gorton, O.K., Bubb, W.A., and Kwan, A.H. (2021). Cancer stem cell characteristics and their potential as therapeutic targets. Med. Oncol. *38*, 76. https://doi.org/10.1007/s12032-021-01524-8.
54. Kumar, R., Pereira, R.S., Zanetti, C., Minciacchi, V.R., Merten, M., Meister, M., Niemann, J., Dietz, M.S., Rüssel, N., Schnütgen, F., et al. (2020). Specific, targetable interactions with the microenvironment influence imatinib-resistant chronic myeloid leukemia. Leukemia *34*, 2087–2101. https://doi.org/10.1038/s41375-020-0866-1.
55. Reuther, J.Y., Reuther, G.W., Cortez, D., Pendergast, A.M., and Baldwin, A.S., Jr. (1998). A requirement for NF-kappaB activation in Bcr-Abl-mediated transformation. Genes Dev. *12*, 968–981. https://doi.org/10.1101/gad.12.7.968.
56. Stein, S.J., and Baldwin, A.S. (2011). NF-kappaB suppresses ROS levels in BCR-ABL(+) cells to prevent activation of JNK and cell death. Oncogene *30*, 4557–4566. https://doi.org/10.1038/onc.2011.156.
57. Shen, N., Yan, F., Pang, J., Zhao, N., Gangat, N., Wu, L., Bode, A.M., Al-Kali, A., Litzow, M.R., and Liu, S. (2017). Inactivation of Receptor Tyrosine Kinases Reverts Aberrant DNA Methylation in Acute Myeloid Leukemia. Clin. Cancer Res. *23*, 6254–6266. https://doi.org/10.1158/1078-0432.CCR-17-0235.
58. Li, L., Liu, W., Sun, Q., Zhu, H., Hong, M., and Qian, S. (2021). Decitabine Downregulates TIGAR to Induce Apoptosis and Autophagy in Myeloid Leukemia Cells. Oxid. Med. Cell. Longev. *2021*, 8877460. https://doi.org/10.1155/2021/8877460.
59. Zhu, X.Y., Liu, W., Liang, H.T., Tang, L., Zou, P., You, Y., and Zhu, X.J. (2020). AICAR and Decitabine Enhance the Sensitivity of K562 Cells to Imatinib by Promoting Mitochondrial Activity. Curr. Med. Sci. *40*, 871–878. https://doi.org/10.1007/s11596-020-2266-1.
60. Pashaiefar, H., Izadifard, M., Yaghmaie, M., Montazeri, M., Gheisari, E., Ahmadvand, M., Momeny, M., Ghaffari, S.H., Kasaeian, A., Alimoghaddam, K., and Ghavamzadeh, A. (2018). Low Expression of Long Noncoding RNA IRAIN Is Associated with Poor Prognosis in Non-M3 Acute Myeloid Leukemia Patients. Genet. Test. Mol. Biomarkers *22*, 288–294. https://doi.org/10.1089/gtmb.2017.0281.
61. Hassn Mesrati, M., Syafruddin, S.E., Mohtar, M.A., and Syahir, A. (2021). CD44: A Multifunctional Mediator of Cancer Progression. Biomolecules *11*, 1850. https://doi.org/10.3390/biom11121850.
62. Mendonça, L.S., Firmino, F., Moreira, J.N., Pedroso de Lima, M.C., and Simões, S. (2010). Transferrin receptor-targeted liposomes encapsulating anti-BCR-ABL siRNA or asODN for chronic myeloid leukemia treatment. Bioconjug. Chem. *21*, 157–168. https://doi.org/10.1021/bc9004365.
63. Rothe, K., Babaian, A., Nakamichi, N., Chen, M., Chafe, S.C., Watanabe, A., Forrest, D.L., Mager, D.L., Eaves, C.J., Dedhar, S., and Jiang, X. (2020). Integrin-Linked Kinase Mediates Therapeutic Resistance of Quiescent CML Stem Cells to Tyrosine Kinase Inhibitors. Cell Stem Cell *27*, 110–124.e9. https://doi.org/10.1016/j.stem.2020.04.005.
64. Dobin, A., Davis, C.A., Schlesinger, F., Drenkow, J., Zaleski, C., Jha, S., Batut, P., Chaisson, M., and Gingeras, T.R. (2013). STAR: ultrafast universal RNA-seq aligner. Bioinformatics *29*, 15–21. https://doi.org/10.1093/bioinformatics/bts635.
65. Trapnell, C., Williams, B.A., Pertea, G., Mortazavi, A., Kwan, G., van Baren, M.J., Salzberg, S.L., Wold, B.J., and Pachter, L. (2010). Transcript assembly and quantification by RNA-Seq reveals unannotated transcripts and isoform switching during cell differentiation. Nat. Biotechnol. *28*, 511–515. https://doi.org/10.1038/nbt.1621.
66. Law, C.W., Chen, Y., Shi, W., and Smyth, G.K. (2014). voom: Precision weights unlock linear model analysis tools for RNA-seq read counts. Genome Biol. *15*, R29. https://doi.org/10.1186/gb-2014-15-2-r29.
67. Iioka, H., Loiselle, D., Haystead, T.A., and Macara, I.G. (2011). Efficient detection of RNA-protein interactions using tethered RNAs. Nucleic Acids Res. *39*, e53. https://doi.org/10.1093/nar/gkq1316.
68. Gagliardi, M., and Matarazzo, M.R. (2016). RIP: RNA Immunoprecipitation. Methods Mol. Biol. *1480*, 73–86. https://doi.org/10.1007/978-1-4939-6380-5_7.
69. Lou, J., Hao, Y., Lin, K., Lyu, Y., Chen, M., Wang, H., Zou, D., Jiang, X., Wang, R., Jin, D., et al. (2020). Circular RNA CDR1as disrupts the p53/MDM2 complex to inhibit Gliomagenesis. Mol. Cancer *19*, 138. https://doi.org/10.1186/s12943-020-01253-y.

STAR★METHODS

KEY RESOURCES TABLE

REAGENT or RESOURCE	SOURCE	IDENTIFIER
Antibodies		
CD44 Rabbit mAb	Abcam	Cat# ab157107; RRID: AB_2847859
CD34 FITC	BD Biosciences	Cat#555821; RRID: AB_396150
FITC Isotype Control Antibody	Bioegend	Cat#400633; RRID: AB_893678
CD44 PE-Cy7	BD Biosciences	Cat#560533; RRID: AB_1727483
PE-Cy7 Isotype Control Antibody	BD Biosciences	Cat#560542; RRID: AB_1727595
NF-kappaB p65 Rabbit mAb	Cell Signaling Technology	Cat#8242S; RRID: AB_10859369
Rabbit mAb Isotype Control	Cell Signaling Technology	Cat#3900S; RRID: AB_1550038
Phospho-NF-κB p65 Rabbit mAb	Cell Signaling Technology	Cat#3033S; RRID: AB_331284
GAPDH Rabbit polyAb	Proteintech	Cat#10494-1-AP; RRID: AB_2263076
Anti-mouse IgG, HRP-linked mAb	Cell Signaling Technology	Cat#7076S; RRID: AB_330924
HRP Goat Anti-Rabbit IgG	Abclonal	Cat#AS014; RRID: AB_2769854
Chemicals, peptides, and recombinant proteins		
Imatinib Mesylate	Sigma Aldrich	Cat# 220127-57-1
Decitabine	Sigma Aldrich	Cat#A3656-5mg
BAY11-7082	APExBIO	Cat#A4210
Human Recombinant IL-3	STEMCELL Technologies	Cat#78040
Human Recombinant IL-6	STEMCELL Technologies	Cat#78050
Human Recombinant G-CSF	STEMCELL Technologies	Cat#78012
BIT 9500 Serum Substitute	STEMCELL Technologies	Cat#09500
2-Mercaptoethanol	Sigma Aldrich	21985023; Cas:60-24-2
Puromycin Dihydrochloride	Solarbio	Cat#IP1280
Iscove's Modified Dulbecco's Medium	Biological Industries	Cat#01-058-1A
Propidium Iodide	Sigma Aldrich	P4170; Cas25535-16-4
RNase A	Beyotime Biotechnology	Cat#ST576
Certified Fetal Bovine Serum (FBS)	Biological Industries	Cat#04-001-1ACS
White Egg Avidin	Sigma Aldrich	189725; Cas1405-69-2
Ribonucleic Acid from Baker's Yeast	Sigma Aldrich	R6750; Cas63231-63-0
Magnesium Chloride Solution	Sigma Aldrich	M1028; Cas7786-30-3
5×Annealing Buffer	Beyotime Biotechnology	Cat#R0051
HEPES PH7.0	Jisskang	Cat#JR0086
Nonidet TM P40 Substitute	Soalrbio	N8030-100
RNase Inhibitor/RNasin	Promega	Cat#N2115
ROX Dye (20 μM)	Accurate Biology	Cat#AG11703
SDS-PAGE Protein Loading Buffer (5X)	Beyotime Biotechnology	Cat#P0015L
QuickBlock™ Western Primary Antibody Diluent	Beyotime Biotechnology	Cat#P0256
5×G250 (Protein Quantitative Analysis)	Solarbio	Cat#PC0015
RIPA's Lysate (strong)	Beyotime Biotechnology	Cat#P0013B
Phenylmethylsulfonyl Fluoride, PMSF	Beyotime Biotechnology	Cat#ST506
Phosphatase Inhibitor Cocktail II (100× in ddH_2O)	MedChemExpress	Cat#HY-K0022
Tricolor Prestained Protein Marker 10kDa~250kDa	Epizyme	Cat#WJ103

(*Continued on next page*)

Continued

REAGENT or RESOURCE	SOURCE	IDENTIFIER
Critical commercial assays		
Plasmid Flute Kit	TIANGEN	Cat#DP103
In-Fusion® HD Cloning Kit	TakaRa	Cat#639650
AmpliScribe™ T7-Flash™ Transcription Kit	Epicentre	Cat#ASF3507
Protein A/G Magnetic Beads	Bimake	Cat #B23202
T4 DNA Ligase	Promega	Cat#M1801
SYBR Green Pro Taq HS Premixed qPCR Kit	Accurate Biology	Cat#AG11701
Lipofectamine™ 2000 Transfection Reagent	Thermo Fisher Scientific	Cat#11668-019
Opti-MEM™ I Minus Serum Medium	Thermo Fisher Scientific	Cat# 31985062
Dynabeads MyOne Streptavidin C1	Thermo Fisher Scientific	Cat#35002D
Cell Counting Kit-8	APE×BIO	Cat#K1018
EasySep Human CD34 Pos Selection Kit II	STEMCELL Technologies	Cat# 17856
Tanon™ ECL Chemiluminescent Substrate	Tanon	Cat#180-5001
Evo M-MLV Reverse Transcription Kit with gDNA Removal Reagent for qPCR	Accurate Biology	Cat#AG11705
Pro Taq HS Premixed Probe Method qPCR Kit	Accurate Biology	Cat#AG11704
2×Accurate Taq Master Mix (with Dye)	Accurate Biology	Cat#AG11009
Annexin V-AbFluor™ 488/PI Apoptosis Detection Kit	Elabscience	Cat#E-CK-A211
Annexin V-APC/PI Apoptosis Kit	KeyGEN BioTECH	Cat#KGA1030-50
EasyPure® Quick Gel Extraction Kit	TransGen Biotech	Cat#EG101
QIAquick Gel Extraction Kit	QIAGEN	Cat#28704
TRIzol	Accurate Biology	Cat#AG21101
NEBNext® Ultra™ RNA Library Prep Kit for Illumina®	NEB	Cat#E7530L
MethoCult™ H4100	STEMCELL Technologies	Cat#04100
Deposited data		
IRAIN-overexpressed K562 cells compared to Vector-control K562 cells	GEO	GEO: GSE263645
Experimental models: Cell lines		
K562	ATCC	Cat#CCL-243; RRID: CVCL_0004
K562/G01	Laboratory of Dr. C. Ji[29]	Cat#CL-0589; RRID: CVCL_4V47
HEK 293T	ATCC	Cat#CRL-3216; RRID: CVCL_0063
MEG-01	ATCC	Cat#CRL-2021; RRID: CVCL_0425
MV4-11	ATCC	Cat#CRL-9591; RRID: CVCL_0064
U937	ATCC	Cat#CRL-1593.2; RRID: CVCL_0007
Oligonucleotides		
Primer GAPDH-Reverse 5′-ACCCTGTTGCTGTAGCCA-3′	This paper	N/A
Primer GAPDH-Forward 5′-CCACTCCTCCACCTTTGAC-3′	This paper	N/A
Primer CD44 Forward 5′- GACAGCAACCAAGAGGCAAG-3′	Godavarthy et al.[16]	N/A
Primer CD44 Reverse 5′-AGACGTACCAGCCATTTGTG-3′	Godavarthy et al.[16]	N/A
Primer ABL Forward 5′-CTAAAGGTGAAAAGCTCCG-3′	This paper	N/A
Primer ABL Reverse 5′- GACTGTTGACTGGCGTGAT -3′	This paper	N/A
Taqman probe ABL 5′- CCATTTTTGGTTTGGGCTTCACACCATT	This paper	N/A
Primer BCR-ABL Forward 5′-TCCGCTGACCATCAATAAGG-3′	This paper	N/A
Primer BCR-ABL Reverse 5′-GGTTTGGGCTTCACACCATTC-3′	This paper	N/A
Primer IRAIN-156-F CGCTCGCAAAACACAACACC	This paper	N/A

(*Continued on next page*)

Continued

REAGENT or RESOURCE	SOURCE	IDENTIFIER
Primer IRAIN-156-R CCGACGTGCATTCCGACACA	This paper	N/A
IRAIN-probe (for IRAIN-156 primer) CTGAAACCACAGCGTACGACACCTCTC	This paper	N/A
Primer IRAIN-138-F CGACACATGGTCCAATCACTGTT	Sun et al.[24]	N/A
Primer IRAIN-138-R AGACTCCCCTAGGACTGCCATCT	Sun et al.[24]	N/A
Primer NF-κB p65-F ACCCCTTCCAAGAAGAGCAG	This paper	N/A
Primer NF-κB p65-R AGATCTTGAGCTCGGCAGTG	This paper	N/A
siRNA sequences of negative control (siNC) AATTCTCCGAACGTGTCACGT	This paper	N/A
siRNA sequences of IRAIN-1 (siIRAIN-1) AAGAGCGACACTGCTTATTAA	This paper	N/A
siRNA sequences of IRAIN-2 (siIRAIN-2) AACCCTTAATGTGGTCCGGTT	This paper	N/A
siRNA sequences of CD44 (siCD44) GCGCAGATCGATTTGAAUATT	This paper	N/A
siRNA sequences of RELA/p65-1(siRELA-1) TCTTCCTACTGTGTGACAATT	This paper	N/A
siRNA sequences of RELA/p65-2(siRELA-2) GCACCATCAACTATGATGATT	This paper	N/A
siRNA sequences of BCR-ABL1(siBCR-ABL1) GCAGAGTTCAAAAGCCCTT	Mendonça et al.[62]	N/A
Software and algorithms		
GraphPad Software 8.0	GraphPad	https://www.graphpad.com
FlowJo (version 10.8.1)	BD Biosciences	https://www.flowjo.com/solutions/flowjo/downloads
CytExpert 2.4	Beckman	https://www.beckman.com/flow-cytometry/research-flow-cytometers/cytoflex/software
7500 Software v2.3	Thermo Fisher Scientific	https://www.thermofisher.cn/cn/zh/home/technical-resources/software-downloads

RESOURCE AVAILABILITY

Lead contact

Further information and requests for resources and reagents should be direct to and will be fulfilled by the lead contact, Dr. Jinsong Yan (yanjsdmu@dmu.edu.cn).

Materials availability

This study did not generate new unique reagents. All plasmids generated in this study were accessible from the lead contact with a completed material transfer agreement.

Data and code availability

- All RNA-seq raw data can be accessed at the Gene Expression Omnibus under the accession numbers: GEO:GSE263645.
- This paper does not report original code.
- Any additional information for reanalyzing the data in this study is available from the lead contact upon request.

EXPERIMENTAL MODEL AND STUDY PARTICIPANT DETAILS

Bone marrow samples were obtained from 17 patients with newly diagnosed CML (6 female and 11 male patients), 30 patients with AML (12 female and 18 male patients), and 15 healthy volunteers (10 female and 5 male). Information of human participant was listed in Table S1. Patients with *BCR-ABL1* kinase domain mutations were excluded from the study. This study was approved by the Institutional Review Board and Ethics Committee of the Second Hospital of Dalian Medical University in China, and the ethical approval number is 2023-XWLW-01, and all participants provided written informed consent.

Cell culture

Bone marrow mononuclear cells (BMMNC) from CML patients were isolated using Ficoll-Paque gradient centrifugation (TBD). The $CD34^+$ cells were immunomagnetically enriched according to the instructions of the EasySep CD34 Positive Selection Kit (STEMCELL Technologies), and their purity was detected using a FITC-labeled anti-CD34 antibody by flow cytometry. As described elsewhere,[63] the enriched $CD34^+$ and mononuclear cells were cultured in Iscove's modified Dulbecco's medium (IMDM) supplemented with Serum Substitute BIT 9500 (STEMCELL Technologies), 10^{-4} M 2-mercaptoethanol, 20 ng/mL IL-3, 20 ng/mL IL-6, 100 ng/mL Flt3-ligand, and 20 ng/mL granulocyte colony-stimulating factor (STEMCELL Technologies), in a humidified atmosphere at 37°C, with 5% CO_2.

The human cell lines K562, MEG-01, U937, MV4-11, and HEK293T were purchased from the American Type Culture Collection. The K562/G01, an induced imatinib-resistant cell line from K562, was kindly donated by Dr. C.Y. Ji (Qilu Hospital, Shandong University, China).[29] The K562 and K562/G01 cells were cultured in IMDM (VivaCell Biosciences), and K562/G01 cells were added with 1 μM imatinib to maintain its resistance to TKI, and imatinib was removed from the culture medium of K562/G01 cells for at least 72 h before experiments. The U937, MV4-11, and MEG-01 cells were cultured in RPMI-1640 (VivaCell Biosciences) supplemented with 10% fetal bovine serum (Thermo Fisher Scientific), 100 U/mL penicillin and 0.1 mg/mL streptomycin. The HEK293T cells were cultured in Dulbecco's modified Eagle's medium (DMEM) (VivaCell Biosciences). All cell lines were cultured in a humidified atmosphere at 37°C, with 5% CO_2.

METHOD DETAILS

Agents and drugs

A stock solution of imatinib (Sigma-Aldrich) was dissolved in water, and decitabine (Sigma-Aldrich) and BAY11-7082 (APExBIO) were dissolved in dimethyl sulfoxide (DMSO). All stock solutions were stored at -20°C.

Lentiviral plasmid construction

The Lentiviral plasmid pCDH-CMV-MCS-EF1-CopGFP-T2A-Puro-*IRAIN* (pCDH-*IRAIN*) and lentiviral vector pCDH-CMV-MCS-EF1-CopGFP-T2A-Puro (pCDH-Vector) were used for *IRAIN* overexpression and the control plasmid, respectively. They were kindly donated by Dr. J. Sun (Stem Cell and Cancer Center, First Affiliated Hospital, Jilin University, China).[24] The lentiviral vector pLKO.1-puro (Addgene, #8453) was used to construct plasmids for *IRAIN* knockdown according to the manufacturer's protocols (https://www.addgene.org/protocols/plko/). The oligonucleotide sequences of shRNA targeting *IRAIN* were 5′-AACCCTTAATGTGGTCCGGTT-3′ and for negative control–shRNA 5′-AATTCTCCGAACGTGTCACGT-3′. In detail, the pLKO.1-puro vector was linearized by restriction enzymes Age I and EcoR I and then was extracted using EasyPure® Quick Gel Extraction Kit (TransGen Biotech). The linearized pLKO.1-puro vector was ligated with the annealed oligonucleotide of shRNAs or shNC, with T4 DNA ligase (Promega) at 16°C overnight. The constructed plasmid, pLKO.1-puro, expressing shRNA and targeting *IRAIN* was abbreviated to sh*IRAIN*, and that expressing the negative control, shRNA, was abbreviated to shNC.

Lentivirus production

According to a previously described protocol,[63] lentiviruses were produced by transfecting 293T cells with a lentiviral plasmid, packaging the plasmid psPAX2 (Addgene, #12260), or enveloping plasmid pMD2G (Addgene, #12259) using Lipofectamine 2000 (Thermo Fisher Scientific). A total of 5×10^6 293T cells were plated in 6-cm Falcon tissue culture dishes in 5 mL DMEM supplemented with 10% FBS 24 h before transfection. Before transfection, 3.5 mL of DMEM was refreshed per dish. The detailed procedure of preparation for the transfection mixtures using two sterile tubes was as follows: the plasmid mixture consisting of 2 μg lentiviral plasmid, 1.5 μg psPAX2, and 1.5 μg pMD2G was added with Opti-MEM medium (Thermo Fisher Scientific) to a total volume of 250 μL in one sterile tube for each 5-cm dish. Then, 20 μL of Lipofectamine 2000 was mixed with 230 μL of Opti-MEM medium (Thermo Fisher Scientific) in another sterile tube. The tubes were incubated for 5 min at room temperature. The contents of the two tubes were merged for a 20-minute incubation at room temperature. Finally, the transfection mixture was added to 293T cells for 6 h and then supplemented with 10% FBS in the cultured medium of 293T cells. Forty-eight hours after transfection, the viral supernatant was collected and filtered with a 0.44 μm polyether sulfone filter, followed by an ultracentrifugation to concentrate the virus particles. The virus particle pellet was resuspended in 1 mL DMEM containing 5% DNase under gentle agitation for 1 h at room temperature. Multiple aliquots of the concentrated virus were stored at -80°C until use.

Lentivirus-mediated *IRAIN* overexpression or knockdown in CML cells

The myeloid leukemia cell lines K562/G01, MEG-01, U937, and MV4-11cells were utilized to establish stable *IRAIN*-overexpressing sublines. According to the protocol provided by Rothe et al.,[63] 5×10^5 myeloid leukemia cells in 2 mL of completed medium were seeded into each well of a 6-well plate and then were supplemented with 100 μL of concentrated lentivirus particles either containing constructs overexpressing *IRAIN* or an empty vector. After 48 h, the myeloid leukemia cells were washed with PBS and refreshed with a complete medium containing 2 mg/mL puromycin. The K562/G01 cells infected with the vector lentivirus or *IRAIN*-expressing lentivirus were named K562/G01 Vector and K562/G01 *IRAIN*, respectively. The MEG-01 cells transfected with the same agents were named MEG-01 Vector and MEG-01 *IRAIN*. The U937 cells transfected with the same agents were named U937 Vector and U937 *IRAIN*, and the MV4-11 cells were named MV4-11 Vector and MV4-11 *IRAIN*, respectively.

BMMNCs or purified $CD34^+$ cells sorted from BMMNCs of CML patients were separately transfected with the vector lentivirus or *IRAIN*-overexpressed lentivirus. They were incubated for over 48 h and then utilized for further assays *in vitro*. To establish stable sublines with knockdown of *IRAIN* expression, K562, and MEG-01 cells were transfected with lentivirus particles containing the lentivirus vector (shNC) or shRNA constructs targeting human *IRAIN* (sh*IRAIN*). The K562 cells infected with shNC or sh*IRAIN* were named K562 shNC and K562 sh*IRAIN*, and MEG-01 cells that were infected with the same agents were named MEG-01 shNC or MEG-01 sh*IRAIN*, respectively.

Knockdown of *IRAIN* with small interfering RNAs

To knockdown *IRAIN* with small interfering RNAs (siRNAs) in the BMMNCs of primary CML blasts or myeloid leukemia cell lines, siRNAs were transiently transfected using Lipofectamine 2000 reagent (Thermo Fisher Scientific), according to the manufacturer instructions.[62] Cells (1×10^6) suspended in 1.3 mL of serum-free medium were seeded in each well of a 6-well plate. A siRNA-lipid mixture was prepared by mixing 200 pmol siRNA with Opti-MEM medium (Thermo Fisher Scientific) to reach a total volume of 250 μL for the transfection of each well. In a separate tube, 10 μL of Lipofectamine 2000 was mixed with 240 μL of Opti-MEM medium (Thermo Fisher Scientific) and then incubated with the mixture for 20 minutes at room temperature before adding dropwise into cells. After 6 h, 10% FBS was supplemented into the infected cells for a continuing culture. The K562 cells transiently transfected with either the siRNA or the negative control siRNA to knock down *IRAIN* were named K562 siIRAIN and K562 siNC, respectively. Similarly, the MEG-01 cells were named MEG-01 siIRAIN and MEG-01 siNC, respectively. The K562 cells transiently transfected with siRNA or a negative control siRNA to knockdown CD44 were named K562 siCD44 and K562 siNC, and the MEG-01 cells treated similarly were named MEG-01 siCD44 and MEG-01 siNC, respectively.

Cell proliferation and viability

The cells were seeded at a density of 3,0000 cells/mL in 96-well plates and were cultured for 0, 24, 48, 72 h in a humidified atmosphere at 37°C, with 5% CO_2. Then approximately 10 μL of CCK8 solution (APE × BIO) was added to each well. After 4 h of incubation at 37°C, the absorbance of OD value at a 450 nm wavelength reflecting viable cell counts was detected using a BioTek ELX800 universal microplate reader (BioTek Instruments, Inc.). The cell proliferation rates were calculated as the relative absorbance by dividing the absorbance at time points of 24, 48, and 72 h by the absorbance at 0 h. The cell viability was calculated as the percentage of cell counts in the drug-treated group compared to the control group. The IC_{50} values were calculated using logistic non-linear regression.

Colony forming assays

Single-cell suspension at a density of 2000 cells/ml were dispersed into each well in 24-well tissue culture plates, which contains complete medium (RPMI-1640 medium supplemented with 10% FBS, 1% penicillin and streptomycin) mixed with methylcellulose (STEMCELL Technologies, H4100) according to manufacture instructions.[17] Cells were incubated in a humidified atmosphere at 37°C, with 5% CO_2. Colonies (> 50 cells) were determined after 14 days in culture using telescope (leica). All analysis were performed in triplicate.

Apoptosis detection

According to the manufacturer's instructions, the harvested cells were washed with PBS, stained with the Annexin V-APC/PI Apoptosis Detection Kit (KeyGEN BioTECH) or Annexin V-FITC/PI Apoptosis Detection Kit (Elabscience) at room temperature for 15 minutes, and detected using a CytoFLEX flow cytometer (Beckman Coulter). The proportion of specific apoptosis induced by drug = [apoptosis cells in treated cells (%) - apoptosis in control cells (%)] / viable control cells (%) ×100%.[34]

Cluster of differentiation assay with flow cytometry

To assess the cluster of differentiation of CD34 or CD44 on the cell surface, cells were stained with anti-CD34 FITC (BD Pharmingen, #555821) or anti-CD44 PE-Cy7 (BD Biosciences, #560533) at a dilution of 1:100 in PBS and incubated in the dark at room temperature for 15 minutes, washed with PBS twice, and detected and analyzed using a CytoFLEX flow cytometer (Beckman Coulter).

Whole transcriptome sequencing

According to the manufacturer's instructions, total RNAs were extracted from the K562-Vector and K562-*IRAIN* cells using TRIzol (Accurate Biology). RNA quality was assessed using the Agilent 2100 Bioanalyzer (Agilent Technologies), and the RNA library was prepared with the NEBNext® Ultra™ RNA Library Prep Kit for Illumina® (NEB), according to the manufacturer's protocol. Paired-end libraries were sequenced

on an Illumina NovaSeq6000 platform (150-nt read length; Novogene Co., Ltd.). Gene annotation format file (GTF, release 27) downloaded from GENCODE website (https://www.gencodegenes.org/) and fasta files corresponding to human reference genome hg38 were fed to STAR aligner (version 2.5.3a).[64] Through the suggested two-pass mapping pipeline of STAR, bam files which label the chromosome position of sequencing reads were obtained. Next, expression abundances of gene-level were measured as Reads Per Kilobase per Million mapped reads (RPKM) using the "cuffnorm" command from the Cufflinks package[65] with the GTF27 file. Differential gene expression analysis comparing K562-*IRAIN* vs. K562-Vector groups was performed as follows using R (http://cran.r-project.org/, v3.6). The lmFit, eBayes, and topTable functions from R package "limma-voom"[66] were performed to the gene expression matrix from Cufflinks. This analysis generated log fold-change and Benjamini-Hochberg-adjusted *P* values for each gene, and genes with fold change (FC) > 1 and *p*-value < 0.05 were classified into the significant differential list. Volcano plot was drawn using the "ggplot2" R package (v3.2.1).

Polymerase chain reaction

The total RNAs were extracted using TRIzol (Accurate Biology), and cDNA was synthesized using a Reverse Transcription Kit (Accurate Biology, #AG11705), according to the manufacturer's instructions. The real-time quantitative PCR was performed using a SYBR Green Premix qRT-PCR Kit (Accurate Biotechnology) in an ABI-7500 Real-Time PCR system (Life Technologies). It was performed for 40 cycles of 95°C for 10 s and 60°C for 30 s, followed by thermal denaturation. The expression of the target gene relative to (Glyceraldehyde-3-phosphate dehydrogenase) GAPDH mRNA was determined using the $2^{-\Delta\Delta Ct}$ method. The primer sequences are listed in the key resources table.

Western blotting

The whole-cell lysates were prepared using a commercial radioimmunoprecipitation assay (RIPA) lysis buffer (Beyotime Biotechnology) supplemented with a protease inhibitor cocktail and phosphatase inhibitor and then boiled in a loading buffer for ten minutes. The denatured proteins were subjected to SDS-PAGE and transferred to a methanol-fixed polyvinylidene difluoride membrane (PVDF). The PVDF membranes were blocked with 5% bovine serum albumin diluted in Tris-buffered saline buffer and supplemented with 0.1% Tween 20 (TBS-T). The membrane was probed overnight at 4°C using the specific primary antibody, then washed with TBS-T and further incubated with a peroxidase-conjugated secondary antibody for 1 h at room temperature. The primary antibodies used in this study are as follows: anti-CD44 (Abcam, #ab157107), anti-NF-κB p65 (Cell Signaling Technology, #8242S), anti-phospho-NF-κB p65 (Cell Signaling Technology, #3033S), anti-AKT (Cell Signaling Technology, #2920), anti-GAPDH (Proteintech, #10494-1-AP), and anti-ABL1 (Santa Cruz, #sc-56887) antibodies. All the primary antibodies were diluted to 1:1000 in the dilution buffer (Beyotime Biotechnology). The secondary antibodies were anti-mouse IgG horseradish peroxidase-linked antibody (Cell Signaling Technology, #7076S) and anti-rabbit IgG HRP (Abclonal, #AS014). The secondary antibodies were diluted to 1:8000 in TBS-T. The blots were imaged using a Tanon™ ECL chemiluminescence and assayed by a Tanon-5200 Imaging System.

RNA pull-down assay

RNA pull-down was carried out according to a published protocol.[67] *IRAIN* full-length sense and antisense sequences were cloned into pcDNA3-tRNA scaffolded SA (tRSA) (Addgene, #32200) and named tRSA-*IRAIN*-sense and tRSA-*IRAIN*-antisense, respectively. The two plasmids were separately utilized as templates for the *in vitro* transcription of RNA products using the AmpliScribe T7-Flash Transcription Kit (Epicenter). The transcribed RNA products, including sense and antisense RNAs, were dissolved in TRIzol reagent for extraction. The extracted RNA products were denatured at 65°C for 5 min in the presence of 10 mM HEPES and 10 mM $MgCl_2$, then cooled to room temperature. Per the instruction of Dynabeads MyOne Streptavidin C1 (Thermo Fisher Scientific), 30 μg of denatured RNA products were separately mixed with 60 μL beads, which were pre-washed two times with fresh lysis buffer containing 200 U/mL RNasin. Finally, the binding of denatured RNA products to beads was incubated in 300 mL lysis buffer containing 200 U/mL RNasin on a rotating shaker at 4°C for 20 min. The K562 cells were washed with cold PBS, lysed in lysis buffer (10 mM HEPES, pH 7.0, 200 mM NaCl, 1 % Triton X-100, 10 mM $MgCl_2$, 1 mM DTT, and 1 mM PMSF), and sonicated lightly. After centrifugation for 10 min at 16 000g at 4°C, the supernatant of the lysed K562 cells was transferred to new tubes, blocked by white egg avidin (Sigma Aldrich) and yeast RNA (Sigma Aldrich), incubated on a rotation shaker at 4°C for 20 min, and finally centrifuged again for 10 min at 16 000 g, 4°C. The centrifuged supernatants containing the protein lysates were transferred to new tubes containing 200 U/mL RNasin (Promega), mixed with bead-labeled RNAs, and then incubated for 2 h. The beads were washed five times with fresh lysis buffer, and the proteins captured by the beads were analyzed by western blotting.

RNA immunoprecipitation (RIP) assay

RIP was carried out according to a published protocol.[68,69] The RIP lysis buffer contained 25 mM Tris-HCl at pH 7.4, 150 mM NaCl, 1 mM EDTA, 1% NP-40, and 5% glycerol. The K562 cells were crosslinked with 0.5% formaldehyde for 10 minutes at room temperature and then lysed in RIP lysis buffer added with DNase I (50 U/mL), RNasin (1000 U/mL), and a protease inhibitor cocktail. The K562 lysates were subjected to sonication and then were centrifugated at 16,000 × g for 10 min at 4°C where 50 μL (5%) of the supernatant served as the "input" control and 950 μL was utilized for RNA immunoprecipitation. Approximately 5 μg of anti-NF-kappaB p65 (Cell Signaling Technology, #8242S) and negative control anti-IgG (Cell Signaling Technology, #3900S) were separately added into the supernatant to incubate on a rotating shaker for 4 h at 4°C. Protein A/G magnetic beads (Bimake) were then added for incubation for 2 h at room temperature. The beads were washed with a buffer (25 mM Tris-HCl at pH 7.4, 500 mM NaCl, 1 mM EDTA, 1% NP-40, and 5% glycerol), and then the immunocomplexes of antibody and

RNAs were de-crosslinked at 70°C for 45 min, followed by incubating with 5 μg Proteinase K at 55°C for 1 h. The immunoprecipitated RNAs were extracted using TRIzol and ethanol, and the extracted RNAs were subjected to qRT-PCR analysis. The qRT-PCR results were analyzed as follows.

$\Delta Ct\ [p65] = Average\ Ct\ [p65] - (Average\ Ct\ [Input] - Log_2(Input\ Dilution\ Factor))$

$\Delta Ct\ [IgG] = Average\ Ct\ [IgG] - (Average\ Ct\ [Input] - Log_2(Input\ Dilution\ Factor))$

$Input\ Dilution\ Factor = (fraction\ of\ the\ input\ RNA\ saved)^{-1}$

"Fraction of the input chromatin saved" refers to the proportion of input in the total sample, which is 5% in this experiment.

$\Delta\Delta Ct\ [p65/IgG] = \Delta Ct\ [p65] - \Delta Ct\ [IgG]$.

$Fold\ Enrichment = 2^{-\Delta\Delta Ct\ [p65/IgG]}$.

QUANTIFICATION AND STATISTICAL ANALYSIS

Statistical analysis

The statistical significance between the two groups was assessed using an unpaired Student's t-test. The one-way analysis of variance (-ANOVA) was used to analyze more than two groups. The GraphPad Prism 8 (GraphPad Software, La Jolla, CA, USA) was used for the statistical analyses. Unless otherwise stated, the data were presented as mean ± SEM (standard error of the mean) for biological triplicates. The *p*-value was set at $p < 0.05$, indicating a significant difference. Further statistical details, including n values, are provided in the figure legends.